# Discharge Measurements Using a Broad-Band Acoustic Doppler Current Profiler

*By* Michael R. Simpson

---

United States Geological Survey
OPEN-FILE REPORT 01-1

8016-20

SACRAMENTO, CALIFORNIA
2001

U.S. DEPARTMENT OF THE INTERIOR
GALE A. NORTON, Secretary

U.S. GEOLOGICAL SURVEY
Charles G. Groat, Director



---

For additional information write to:

District Chief
U.S. Geological Survey
Placer Hall, Suite 2012
6000 J Street
Sacramento, CA 95819-6129

Copies of this report can be purchased from:

U.S. Geological Survey
Information Services
Box 25286
Federal Center
Denver, CO 80225

# CONTENTS

## FIGURES

Chapter 1. Theory of Operation

1.1.–1.40. Graphic illustrations showing:

FIGURES—Continued

FIGURES—Continued

FIGURES—Continued



TABLES

TABLES—Continued



## CONVERSION FACTORS, VERTICAL DATUM, ABBREVIATIONS, AND ACRONYMS

| Multiply | By | To obtain |
|---|---|---|
| centimeter (cm) | 0.3937 | inch (in.) |
| centimeter per second (cm/s) | .3281 | foot per second (ft/s) |
| cubic meter per second ($m^3/s$) | 35.3147 | cubic foot per second ($ft^3/s$) |
| cubic meter per second per second ($m^3/s/s$) | 35.3147 | cubic foot per second per second ($ft^3/s/s$) |
| decibel per meter (dB/m) | .3048 | decibel per foot (dB/ft) |
| decimeter (dm) | 3.937 | inch (in.) |
| kilometer (km) | .6214 | mile (mi) |
| meter (m) | 3.281 | foot (ft) |
| meter per second (m/s) | 3.281 | foot per second (ft/s) |
| millimeter (mm) | .03937 | inch (in.) |
| millimeter per second (mm/s) | .03937 | inch per second (in./s) |
| square meter per second per second ($m^2/s/s$) | 10.7639 | square foot per second per second ($ft^2/s/s$) |

Temperature in degrees Celsius (°C) may be converted to degrees Fahrenheit (°F) as follows:

$$°F = (1.8 \times °C) + 32$$

**Sea level:** In this report, "sea level" refers to the National Geodetic Vertical Datum of 1929 (NGVD of 1929)—a geodetic datum derived from a general adjustment of the first-order level nets of both the United States and Canada, formerly called Sea Level Datum of 1929.

### Abbreviations and Acronyms

| | |
|---|---|
| dB | decibel |
| Hz | hertz |
| hp | horsepower |
| K, kB | kilobyte |
| kHz | kilohertz |
| Mb | megabyte |
| ppt | parts per thousand |
| rpm | revolutions per minute |
| s | second |
| V | volt |
| W | watt |
| AC | alternating current |
| ADCP | acoustic Doppler current profiler |
| ASCII | American standard code for information interchange |
| BB-ADCP | broad-band acoustic Doppler current profiler |
| BNC | bayonet style coaxial |
| CD-ROM | compact disk, read-only memory |
| CFG | configuration (file) |
| CPU | central processing unit |
| CV | coefficient variation |
| DC | direct current |
| DOI | U.S. Department of the Interior |
| EGA | extended graphics array |
| GPS | Global Positioning System |
| IBM | International Business Machines |
| LCD | liquid crystal display |
| LED | luminescent electronic display |
| MS DOS | Microsoft Disk Operating System |
| PC | personal computer |
| QA | quality assurance |
| RDI | R.D. Instruments, Inc. |
| RSSI | reflected signal strength indicator |
| USGS | U.S. Geological Survey |

# Discharge Measurements Using a Broad-Band Acoustic Doppler Current Profiler

*By* Michael R. Simpson

## INTRODUCTION

The measurement of unsteady or tidally affected flow has been a problem faced by hydrologists for many years. Dynamic discharge conditions impose an unreasonably short time constraint on conventional current-meter discharge-measurement methods, which typically last a minimum of 1 hour. Tidally affected discharge can change more than 100 percent during a 10-minute period. Over the years, the U.S. Geological Survey (USGS) has developed moving-boat discharge-measurement techniques that are much faster but less accurate than conventional methods. For a bibliography of conventional moving-boat publications, see Simpson and Oltmann (1993, page 17).

The advent of the acoustic Doppler current profiler (ADCP) made possible the development of a discharge-measurement system capable of more accurately measuring unsteady or tidally affected flow. In most cases, an ADCP discharge-measurement system is dramatically faster than conventional discharge-measurement systems and has comparable or better accuracy. In many cases, an ADCP discharge-measurement system is the only choice for use at a particular measurement site.

ADCP systems are not yet "turnkey"; they are still under development, and for proper operation, require a significant amount of operator training. Not only must the operator have a rudimentary knowledge of acoustic physics, but also a working knowledge of ADCP operation, the manufacturers' discharge-measurement software, and boating techniques and safety.

### Purpose and Scope

The purpose of this report is to describe ADCP operating techniques, fundamental ADCP theory, ADCP discharge-measurement theory, and vessel mounts and operating techniques required for ADCP discharge measurements. It is not intended to replace the "hands-on," USGS-approved training required for all ADCP discharge-measurement system operators. This report only describes the Microsoft Disk Operating System (MS DOS) version of the discharge-measurement software, Transect, and will have to be revised to include future versions that run under Microsoft Windows. The report also only describes the configuration and use of the R.D. Instruments, Inc. (RDI), broad-band ADCP (BB-ADCP). Subsequent modifications to the BB-ADCP will be included in updates to this report if these modifications significantly change the configuration of the ADCP or if discharge-measurement techniques must be changed. This report also will be updated if another manufacturer's ADCP is used to measure discharge by a significant number of USGS users.

### A Short History of Acoustic Doppler Current Profiler Discharge Measurement

In 1982, an ADCP was used to measure the discharge of the Mississippi River at Baton Rouge, Louisiana (Christensen and Herrick, 1982). The test results were encouraging, differing less than 5 percent from simultaneous measurements made with conventional moving-boat methods. However, the computer software and hardware were incapable of processing the velocity data provided by the profiler on a real-time basis; the discharge measurements had to be computed after the fact. Although this technology looked very promising at the time of these tests, computer and Doppler signal-processing technology had not progressed to the level needed to collect and compute reliable river and estuarine discharge measurements.

In 1985, the USGS purchased a narrow-band ADCP to be used for the development of a discharge-measurement system (an explanation of the differences between narrow-band and BB-ADCPs is given in

chap. 1). This discharge-measurement system was successful (Simpson and Oltmann, 1993) but, because of minimum depth limitations, the narrow-band ADCP was usable only in rivers and estuaries with depths greater than 3.4 meters (m) [11.5 feet (ft)].

Because of depth and measurement precision limitations of the narrow-band ADCP, the ADCP manufacturer began exploring a slightly different area of acoustic technology, which has been termed "broad-band." In 1991, a prototype BB-ADCP was developed and tested. The BB-ADCP short-term random error (standard deviation of measured water velocities) was reported to be an order of magnitude lower than that of the narrow-band system and, because of this, could be optimized for shallow-water operation.

The USGS was interested in this technology because of its application to shallow water and purchased one of the first production models of the BB-ADCP from RDI in February 1992 to be evaluated for use in the measurement of river discharge. This evaluation is ongoing in the California District and has been joined by several other districts of the USGS. Morlock (1996) evaluated the BB-ADCP for discharge measurement at selected locations throughout the United States. This evaluation compared discharges measured utilizing a BB-ADCP with discharges measured at 12 stream-gaging sites having stable stage-discharge relations. The results of the evaluation showed that the BB-ADCP system can be used to accurately measure discharge at sites similar to those measured by Morlock (1996).

The manufacturer has since developed smaller versions of the BB-ADCP. Two such instruments are the "Workhorse" with a bottom-tracking option (chap. 1) and the "Rio Grande," which is a Workhorse with built-in bottom-tracking capability. Because the manufacturer has four types of ADCPs capable of measuring river discharge (narrow-band, broad-band, Workhorse, and Rio Grande), they will be referred to as ADCP discharge-measurement systems in this report, and the instrument will be referred to as an ADCP, unless details specific to a particular model are discussed.

The ADCP discharge-measurement system may be the only feasible, accurate method for measuring discharge in tidally affected rivers and estuaries, as well as in rivers or canals with unsteady flow (Simpson and Oltmann, 1993). The ADCP also has proven useful as a substitute for conventional discharge-measurement techniques in many upland rivers with depths too deep for wading measurements.

On the other hand, the setup and operation of the ADCP for discharge measurements is complicated, compared with conventional methods. Configuration of the ADCP for discharge-measurement use requires a working knowledge of conventional discharge-measurement principles, as well as a basic knowledge of acoustics and Doppler shift measurement techniques. With the help of this report, attendance at a USGS-approved ADCP discharge-measurement course, and the manufacturer's documentation, it is hoped that an interested individual can gain the skills needed to accurately measure river discharge using an ADCP.

# CHAPTER 1: THEORY OF OPERATION

## Basic Acoustic Velocity Measurement Principles

Before the operational aspects of an ADCP measurement can be understood, some of the basic physical properties of sound and sound propagation through different mediums must be examined. This chapter introduces basic acoustic Doppler velocity measurement principles and some of the problems associated with such measurements. Much of the information in this chapter was taken from R.D. Instruments, Inc. (1989, 1996).

### The Physics of Sound

What commonly is perceived as sound is a vibration of our eardrums caused by the arrival of pressure waves. The eardrum transfers the pressure-wave information to parts of the inner ear where the mechanical energy of the pressure waves is converted to an electrical signal. The brain interprets this electrical signal as sound.

Sound waves can occur in most media (water, air, and solids) and are similar to water waves; sound waves have crests and troughs that correspond to bands of high and low air pressure, and water waves have crests and troughs that correspond to high and low water-level elevations. Pitch (frequency) of sound waves increases as the wavelength (the distance between the wave peaks) becomes shorter. This frequency, or pitch, usually is expressed in hertz (Hz). One hertz equals one wave (cycle) per second. The human ear can hear frequencies from about 40 Hz to about 24 kilohertz (kHz) (24,000 Hz). These frequencies are dubbed the "sonic" frequencies. Sound frequencies below about 40 Hz are called "subsonic," and sound frequencies above 25,000 Hz are called "ultrasonic."

### The Doppler Principle Applied to Moving Objects

The ADCP uses sound to measure water velocity. The sound transmitted by the ADCP is in the ultrasonic range (well above the range of the human ear). The lowest frequency used by commercial ADCPs is around 30 kHz, and the common range used by the USGS for riverine measurements is between 300–3,000 kHz.

The ADCP measures water velocity using a principle of physics discovered by Christian Johann Doppler (1842) (fig. 1.1). Doppler's principle relates the change in frequency of a source to the relative velocities of the source and the observer. Doppler (1842) stated his principle in the article, "Concerning the Coloured Light of Double Stars and Some Other Constellations in the Heavens," while working in Prague, Czechoslovakia. The Doppler principle can be described best using the water-wave analogy (figs. 1.2, 1.3).

**Figure 1.1.** Christian Johann Doppler.

Figure 1.2 shows a stationary observer watching a series of waves that are passing at a rate of one wave per second. This rate is analogous to a transmit frequency of 1 Hz. In figure 1.3, the wave observer is boating toward the wave source at a rate of four wavelengths per second. Because the waves are passing at a rate of one wave per second, the observer notices the passage of five waves during each second of his boating trip. He senses that the rate of the passing waves is 5 Hz, though the wave source is still emitting waves at 1 Hz. This phenomenon is known as the Doppler effect.

Many people have experienced the Doppler effect while on a busy street. The sound of a car horn seems to drop in frequency as the car passes and recedes from the observer. The apparent lowering of frequency is called the Doppler shift (fig. 1.3). The car is a moving sound-wave source; therefore, when the car is approaching an observer, the frequency of the sound waves striking the observer's ear drums is proportional to the speed of the car (in wavelengths per second) plus the frequency of the car horn in hertz. When the car is receding from the observer, the frequency of the sound waves striking the observer's ear drums is proportional

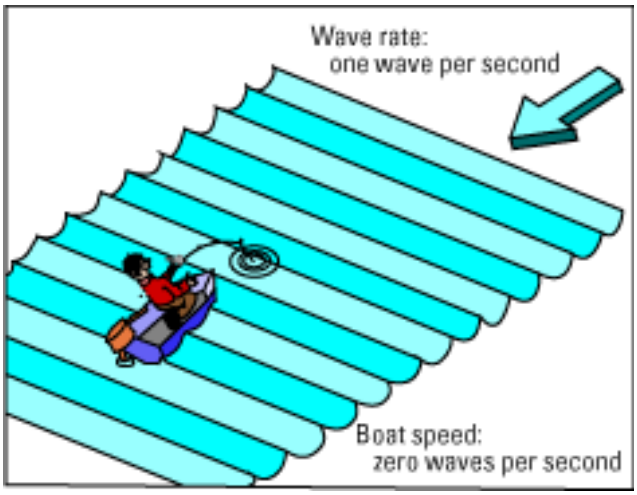


**Figure 1.2.** Stationary wave observer.

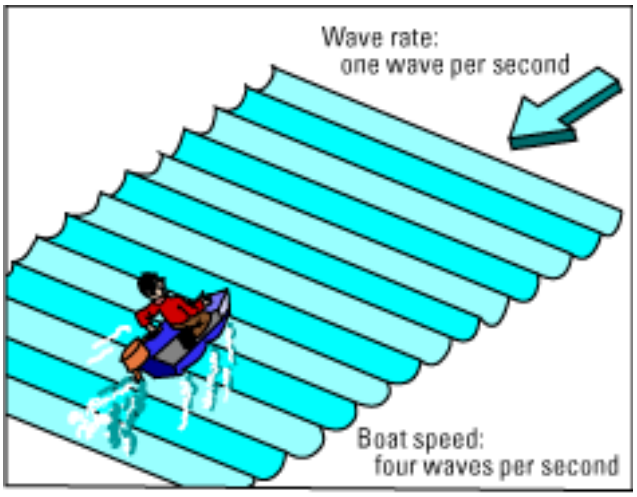


**Figure 1.3.** Moving wave observer.

to the frequency of the car horn (in hertz) minus the speed of the car (in wavelengths per second). If the exact source frequency is known and the observed frequency can be calculated, equation 1.1 can be used to calculate the Doppler shift due to the relative velocities of the source and observer (R.D. Instruments, Inc., 1989):

$$F_D = F_S\left(\frac{V}{C}\right) \qquad (1.1)$$

where

$F_D$ = the Doppler shift frequency, in hertz;

$F_S$ = the transmitted frequency of the sound from a stationary source, in hertz;

$V$ = relative velocity between the sound source and the sound wave receiver (the speed at which the observer is walking toward the sound source), in meters per second; and

$C$ = the speed of sound, in meters per second.

Note that:

- If the observer walks faster ($V$ increases), the Doppler shift ($F_D$) increases
- If the observer walks away from the sound ($V$ is negative), the Doppler shift ($F_D$) is negative
- If the frequency of the sound ($F_S$) increases, the Doppler shift ($F_D$) increases
- If the speed of sound ($C$) increases, the Doppler shift ($F_D$) decreases

### Measuring Doppler Shifts Using Acoustic Backscatter

An ADCP applies the Doppler principle by bouncing an ultrasonic sound pulse off small particles of sediment and other material (collectively referred to as backscatterers) that are present, to some extent, even in optically clear water. A magnified view of the water column and the backscatterers "illuminated" by the sound pulse are shown in figure 1.4. There are, of course, exceptions to every rule, and in tow tanks and some natural rivers, backscatterer density can be too low for the proper operation of an ADCP.

The ADCP transmits an acoustic "ping," or pulse into the water column and then listens for the return echo from the acoustic backscatterers in the water column. Upon receiving the return echo, the ADCP's onboard signal-processing unit calculates the Doppler shift using a form of autocorrelation (the signal is compared with itself later). A schematic diagram of a transmitted acoustic pulse (ping) and the resulting reflected acoustic energy are shown in figure 1.5. Note

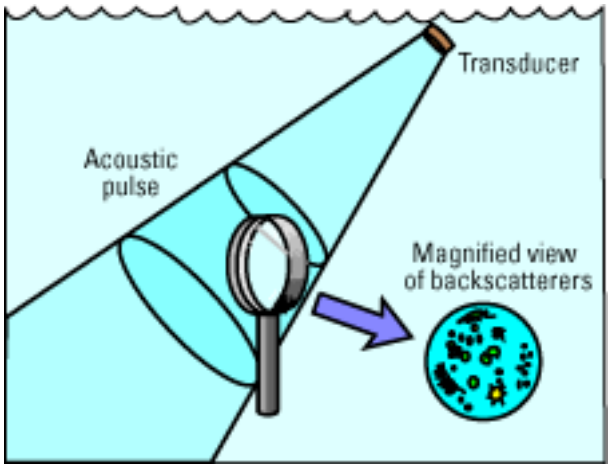


**Figure 1.4.** Magnified view of backscatterers.

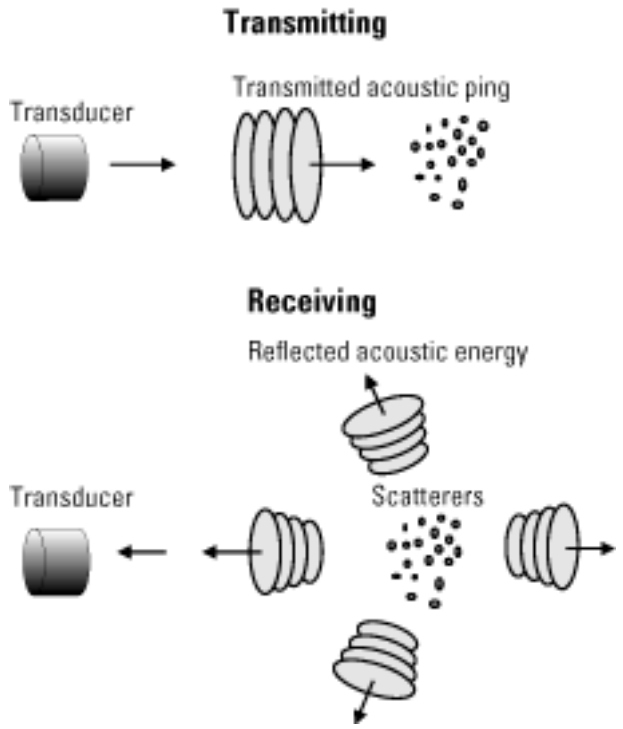


**Figure 1.5.** An acoustic pulse being backscattered.

that very little reflected acoustic energy is reflected back (backscattered) towards the transducer in figure 1.5; most of the acoustic energy is absorbed or reflected in other directions.

#### Measuring Doppler Shifts From a Moving Platform

When the scatterers are moving away from the ADCP, the sound (if it could be perceived by the scatterers) shifts to a lower frequency. This shift is proportional to the relative velocity between the ADCP and the scatterers (fig. 1.5). Part of this Doppler-shifted sound is backscattered towards the ADCP, as if the scatterers were the sound source (fig. 1.6). The sound is shifted one time (as perceived by the backscatterer) and a second time (as perceived by the ADCP transducer) (R.D. Instruments, Inc., 1989).

Because there are two Doppler shifts, equation 1.1 becomes equation 1.2:

$$F_D = 2 F_D \left(\frac{V}{C}\right) \qquad (1.2)$$

If the sound source and receiver move, relative to the Earth, but stay at a fixed distance from one another, there is no Doppler shift. The Doppler shift exists only when sound sources and receivers move in relation to

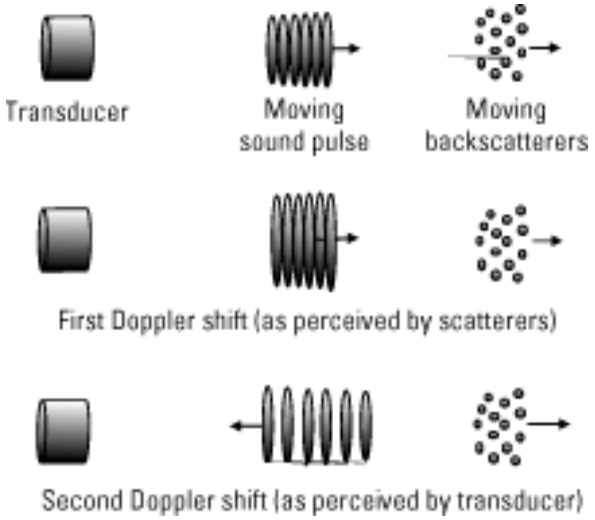


**Figure 1.6.** Reflected pulse showing two Doppler shifts.

each other. The Doppler shift between the source and the Earth exactly cancels the opposite shift between the Earth and the receiver (R.D. Instruments, Inc., 1989).

#### Radial Motion

Only radial motion, which is a change in distance between the source and receiver, will cause a Doppler shift. Figure 1.7 shows 1-second boat tracks in three different directions, relative to the wave source. Boat vector A is parallel with the wave direction; therefore, vector A encounters the full component of Doppler shift. Boat vector B is moving at an angle to the wave direction and encounters only a part of the Doppler shift component, whereas boat vector C (normal to the wave source) encounters no Doppler shift.

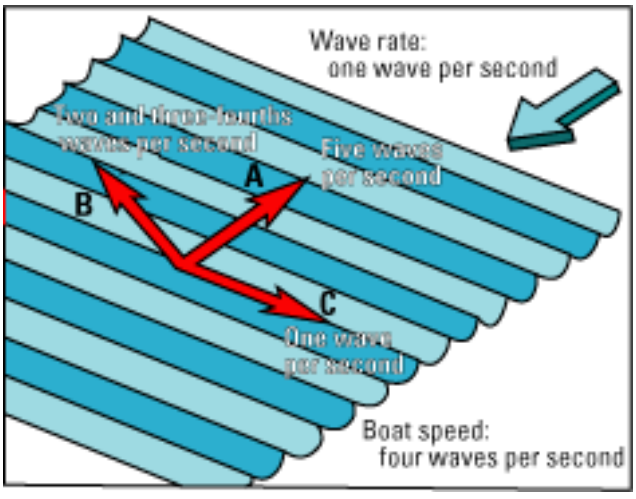


**Figure 1.7.** Effect of radial motion on Doppler shift.

Mathematically, this means the Doppler shift results from the velocity component in the direction of the line between the source and receiver (R.D. Instruments, Inc., 1989) as shown in equation 1.3:

$$F_D = 2F_S\left(\frac{V}{C}\right)\cos(\theta) \qquad (1.3)$$

where

$\theta$ = the angle between the relative-velocity vector and the line between the ADCP and scatterers (fig. 1.8).

## Acoustic Doppler Current Profiler Beam Geometry

### Calculating Three-Dimensional Velocity Components

In a vessel-mounted system, the transducers are mounted near the water surface and aimed downward. Figure 1.9 shows a typical ADCP. Note that there are four independently working acoustic beams with each beam angled 20–30º from the vertical axis of the transducer assembly. This configuration of beams is the so-called "Janus" configuration, named after the Greek God, Janus, who could simultaneously look forward and backward.

### Beam Scenarios

To visualize the three-dimensional capabilities of the "Janus" configuration, refer to figure 1.10 while reading the following scenarios:

- If the starboard (90º left of forward) beam has a positive Doppler shift, the port (90º right of forward) beam has a negative Doppler shift, and the forward and aft beams have no Doppler shift, then the water is flowing from starboard to port (or the water is still and the boat is sliding starboard)
- If the forward beam has a negative Doppler shift, the aft beam has a positive Doppler shift, and the

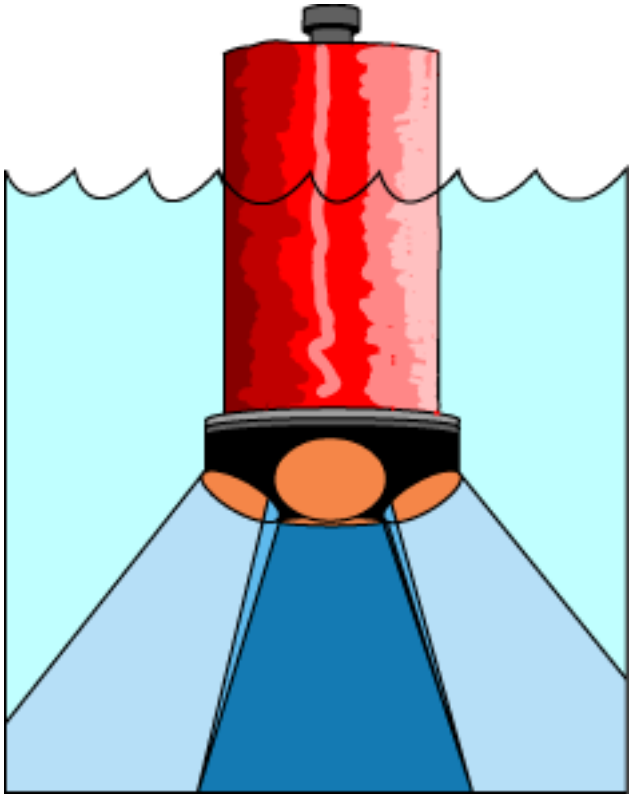

**Figure 1.9.** Downward-looking, convex-head acoustic Doppler current profiler.

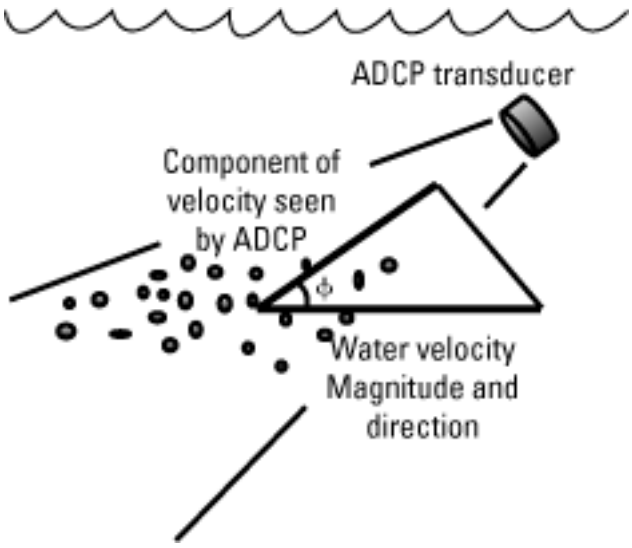


**Figure 1.8.** Velocity components. ADCP, acoustic Doppler current profiler.

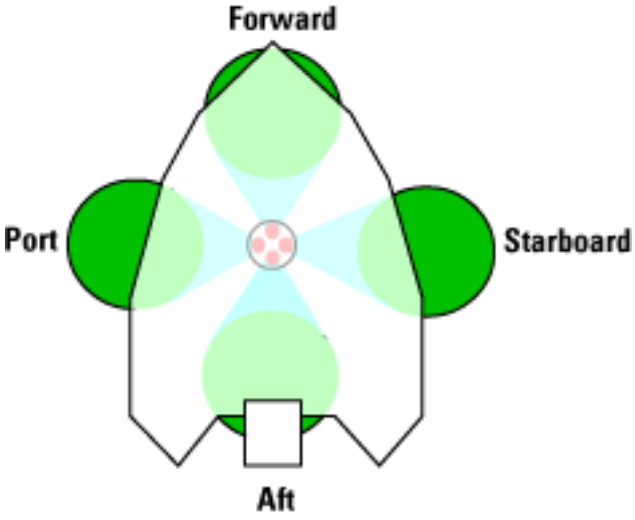


**Figure 1.10.** Boat-mounted acoustic Doppler current profiler with the "Janus" configuration.

starboard and port beams have no shift, then the water is flowing under the boat from aft to forward (or the water is still and the boat is backing)

- If the forward and port beams have a positive Doppler shift of magnitude 1 and the aft and starboard beams have a negative Doppler shift of magnitude 1, then water is passing under the boat from a point halfway between forward and port with a magnitude of the square root of 2, or 1.414 (or the water is still and the boat is crabbing toward the forward port quarter at a magnitude of 1.414)
- If all four beams have a positive Doppler shift, the water is flowing upward toward the hull of the boat (or the water is still and all personnel on the boat should don their life jackets)

The computation of velocity in three dimensions (x, y, z) requires at least three acoustic beams (figs. 1.11 and 1.12). Figure 1.11 shows a northwest-moving water-velocity vector and the resulting Doppler shifts from each of three acoustic beams (a hypothetical, three-beam sonar). Because the water-velocity vector is almost exactly at right angles to beam 2, the resulting Doppler shift on beam 2 is small. The water-velocity vector is approaching and is almost aligned with beam 3; therefore, beam 3 has a large, positive Doppler shift. The water-velocity vector is receding from, and is almost aligned with, beam 1; therefore, beam 1 has a large negative Doppler shift.

Figure 1.12 shows a northeast-moving water-velocity vector. Note that because the water-velocity vector almost is at right angles to beam 3, the resultant Doppler shift is small. The water-velocity vector is approaching beam 1 at an angle; therefore, beam 1 has a large positive Doppler shift. Beam 2 has a large

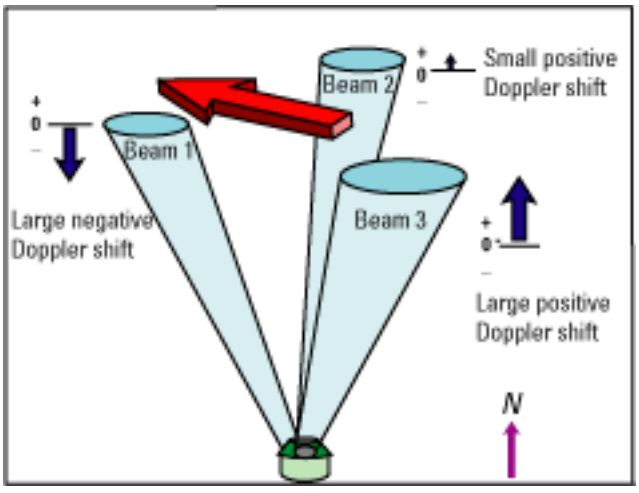


**Figure 1.11.** Northwest-moving water-velocity vector and the resulting Doppler shifts from a hypothetical, three-beam sonar.

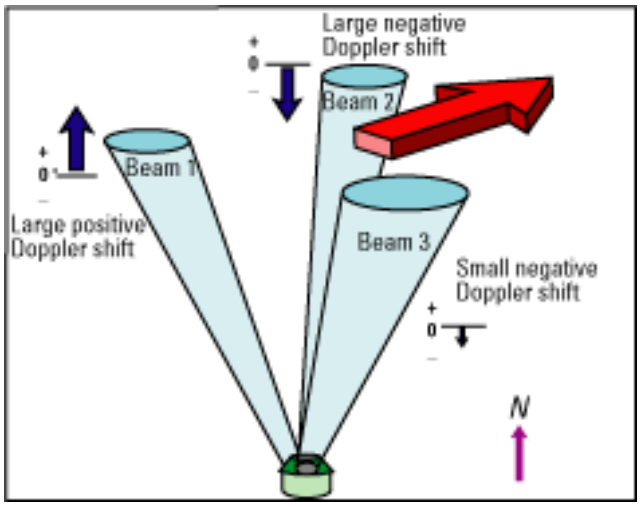


**Figure 1.12.** Northeast-moving water-velocity vector and the resulting Doppler shifts for a hypothetical, three-beam sonar.

negative Doppler shift because the water-velocity vector is receding from, but not perfectly parallel with, beam 2. This configuration also could measure vertical velocities. If all three beams have positive Doppler shifts, then a vertical component of water velocity moving toward the transducers is present. By using simple trigonometry, velocity components in three orthogonal coordinates can be calculated from Doppler shifts measured with three sonar beams.

### The Fourth Beam and Error Calculations

Some ADCP manufacturers use a four-beam configuration and the fourth redundant beam is used to compute an error velocity. This error velocity can be used to test the assumption that flow volume of water bounded by the four measurement beams is homogeneous. Velocity homogeneity means that the water velocities do not change significantly in magnitude or direction within the confines of the acoustic beam footprint. Figure 1.13 shows a homogeneous velocity field bounded by the four beams of an ADCP.

If a velocity field existed as in figure 1.13, the ADCP would provide a nearly zero error velocity. Error velocity is defined as the difference between a velocity measured by one set of three beams versus a velocity measured by the other set of three beams during the same time frame. A difference between these two measurements could be caused by a bad or corrupt beam velocity or by nonhomogeneity (fig. 1.14). In practice, a small error velocity almost always exists because complete homogeneity of the velocity field rarely occurs during field measurements.

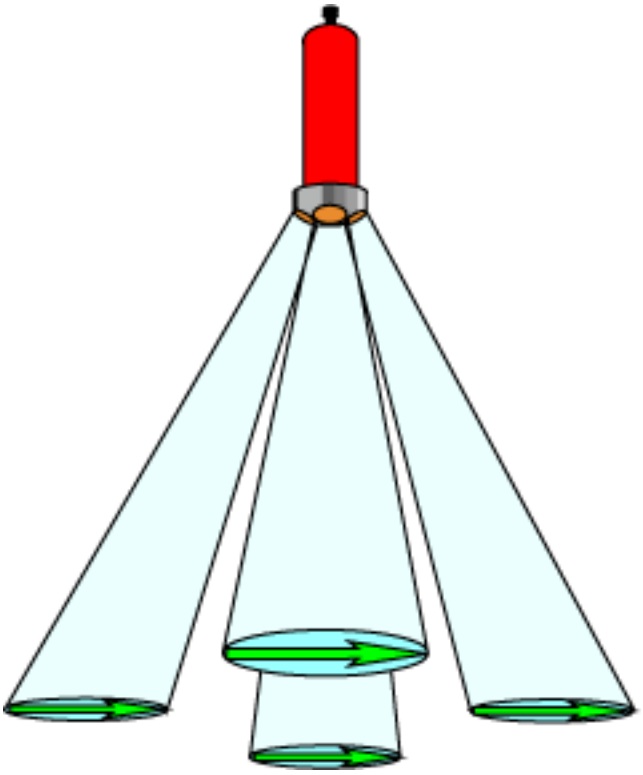

**Figure 1.13.** Acoustic Doppler current profiler measuring a homogeneous velocity field.

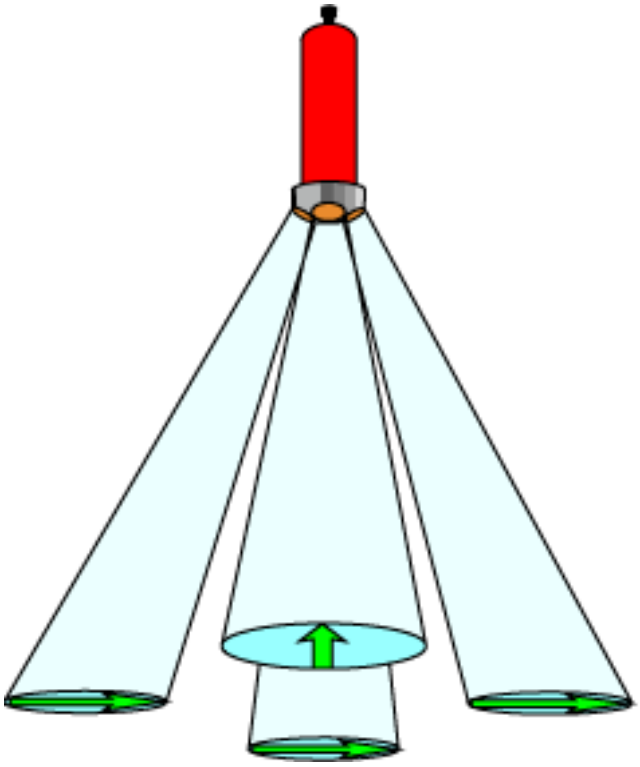

**Figure 1.14.** Nonhomogeneous velocity field bounded by the acoustic Doppler current profiler beams.

## Acoustic Doppler Current Profiler Water-Velocity Profile Measurements

### Acoustic Doppler Current Profiler-Measured Profiles Compared with Conventional Current Meter Measurements

The ADCP is best known for its capability to measure profiles of water velocity. A velocity profile can be compared roughly to using a number of point-velocity meters that are suspended in the vertical axis of a water-velocity field (fig. 1.15). Theoretically, the velocity measured by each conventional current meter is analogous to the velocities measured at the center of ADCP depth cells (fig. 1.15). However, the analogy between a string of current meters and an ADCP profile is not perfect. Current meters measure water velocity at individual points in the vertical profile, whereas velocities that are measured by the ADCP and assigned to individual depth cells are really the center-weighted mean of velocities that are measured throughout the sample window (fig. 1.15).

### Time Gating: Measuring Doppler Shifts from Different Depths

The ADCP profiling capability is accomplished by time gating (and sampling) the received echo at increasingly longer time intervals as the acoustic-beam wave fronts vertically traverse the water column (fig. 1.16).

The analogy of a Navy sonar operator can be used to understand time gating. The sonar operator presses a button on the sonar console causing a “ping” to be transmitted by the ship’s sonar transducer. As soon as the ping is transmitted, the sonar operator activates a stopwatch and begins listening to the returned echo. The sound from the ping travels through the water very

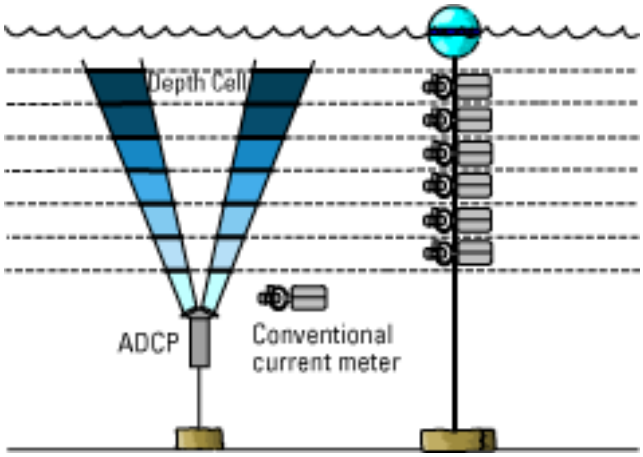


**Figure 1.15.** Analogy of a conventional current-meter string to an acoustic Doppler current profiler (ADCP) profile.

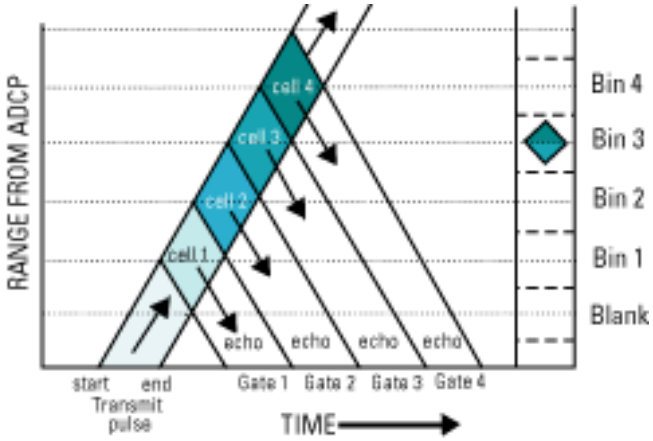


**Figure 1.16.** Acoustic Doppler current profiler (ADCP) time gating. Adapted from R.D. Instruments, Inc., (1989).

fast, but at a finite speed that can be calculated. The operator hears a continuous, low-intensity echo that is caused by the sound reflecting off of particles in the water as the ping speeds toward the ocean floor. The operator hears an abrupt increase in echo amplitude and frequency and immediately presses the stop button on the stopwatch. The echo anomaly was caused by a submerged submarine. The operator then calculates the distance to the submarine using the elapsed time from the stopwatch and a speed-of-sound equation (Urick, 1975). The speed of the submarine, relative to the Navy ship, also can be calculated and is proportional to the Doppler shift of the returned echo.

If the sonar operator was replaced by a computer-controlled receiver and time circuit, the received echo could be recorded and "sliced up" into small pieces with each piece corresponding to a received time. Each slice (depth cell) would be from an increasingly deeper part of the water column. The speed of the particles in each depth cell could be measured by calculating the Doppler shift of the echo in each depth cell. For this purpose, most ADCPs contain a computer-controlled receiver and timer circuit for each acoustic beam, as well as sophisticated signal-processing hardware to calculate Doppler shifts.

The ADCP transmits a ping along each acoustic beam and then time gates the reception of the returned echo on each beam into depth cells. Speed and direction are then calculated (using a center-weighted mean of the velocities measured in the depth cell) and assigned to the center of each depth cell (bin) over the measured vertical.

### Bottom Tracking

To measure absolute water velocities (water velocities relative to the Earth), the ADCP must sense and measure the velocity of the ADCP, relative to the river bottom (bottom tracking). If the velocity of the water is known, relative to the ADCP, and the velocity of the ADCP is known, relative to the river bottom, then the water velocity, relative to the bottom, can be calculated. The bottom-track pulse is somewhat longer than the water-track pulse to properly ensonify the bottom (fig. 1.17). All ADCP instruments that are designed to measure discharge have the ability to calculate vessel velocity using a bottom-track pulse. The bottom-track ping also is used to measure the profiled depth range from each beam. These depth-range measurements are averaged to obtain a depth for the measured velocity profile.

### Acoustic Doppler Current Profiler Limitations for Velocity-Profile Measurements

#### Range Limitations

Reception and calculation of Doppler shift from a returned echo requires sophisticated electronic circuitry as well as high-speed digital signal-processing algorithms. The ADCP contains circuitry and microprocessors capable of resolving very small changes in echo Doppler shift that are needed for accurate water-velocity and bottom-velocity measurement. However, there are some problems associated with echo reception and water-velocity measurement using ADCPs.

In an ADCP, the backscattered echo amplitude falls off as a function of range, frequency, and pulse width, as well as the attenuating properties of the water mass. In ADCP systems, the uncertainty (random error) of the returned velocity measurement is strongly affected by changes in the backscattered echo amplitude. Figure 1.18 shows a spectrograph illustrating the relationship among transmit frequency, echo amplitude, and spectral width. For accurate water-

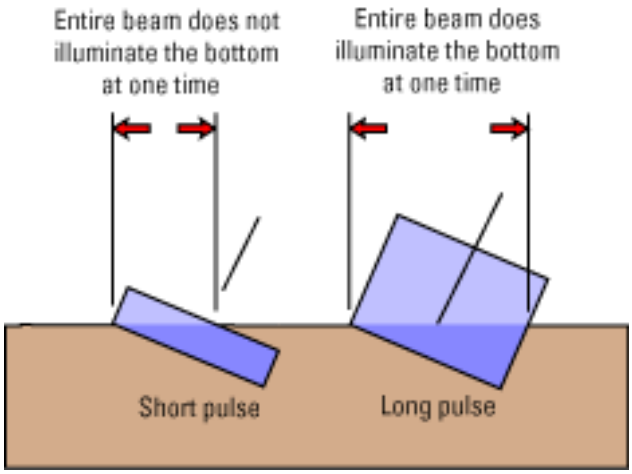


**Figure 1.17.** Short and long bottom-track pulse. Adapted from R.D. Instruments, Inc., (1989).

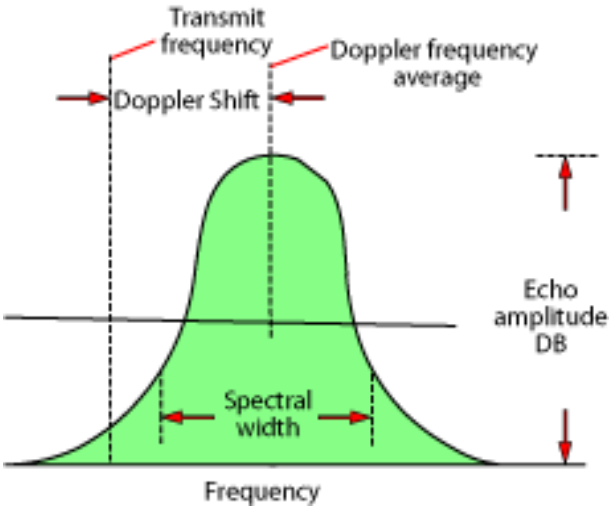


**Figure 1.18.** Spectrograph of received Doppler signal. DB, decibels.

velocity measurement, the returned signal should have a very small spectral width (as shown by the dotted line labelled "Doppler frequency average" in figure 1.18), but, in reality, there are several factors that "spread" or "smear" the returned frequencies over a larger part of the frequency spectrum, as bounded by the solid line in figure 1.18.

The first factor is the finite duration of the acoustic transmit pulse. If the pulse is t seconds long, the reflected signal has a frequency spread of 1/t Hz, about the center frequency (Urick, 1975). This effect is the dominant source of spectral spreading of the received Doppler shifted echo. This spectral spreading causes increased random error in the determination of Doppler shift and, therefore, increased random error in the measurement of water velocity. The smaller the pulse width, the greater the amount of random error.

Figure 1.19 shows a signal being backscattered from scatterers of different sizes that are moving at different speeds, which results in the arrival of signals at differing phases. Because the autocorrelation technique needs accurate phase information to calculate frequency shift, this spreading effect causes random error in the determination of Doppler shift.

In natural waters, the reflected signal is affected significantly by scatterer velocities in the cloud of particulate matter that is "illuminated" by the ultrasonic pulse (fig. 1.20). The result of this cloud-scattering effect is to increase the spectral width of the return signal.

Although the dominant source of spectral spreading is the transmit pulse length, the measured spectral width can be an indicator of velocity uncertainty. As the signal-to-noise ratio decreases near the end of the profile, the spectral width increases. This increase translates directly into velocity uncertainty. Thus, changes in spectral width are related to velocity uncertainty, especially in the last one-third of the profiling range (R.D. Instruments, Inc., 1989).

The echo amplitude is the measure of the energy in the echo and varies with a dynamic range of many

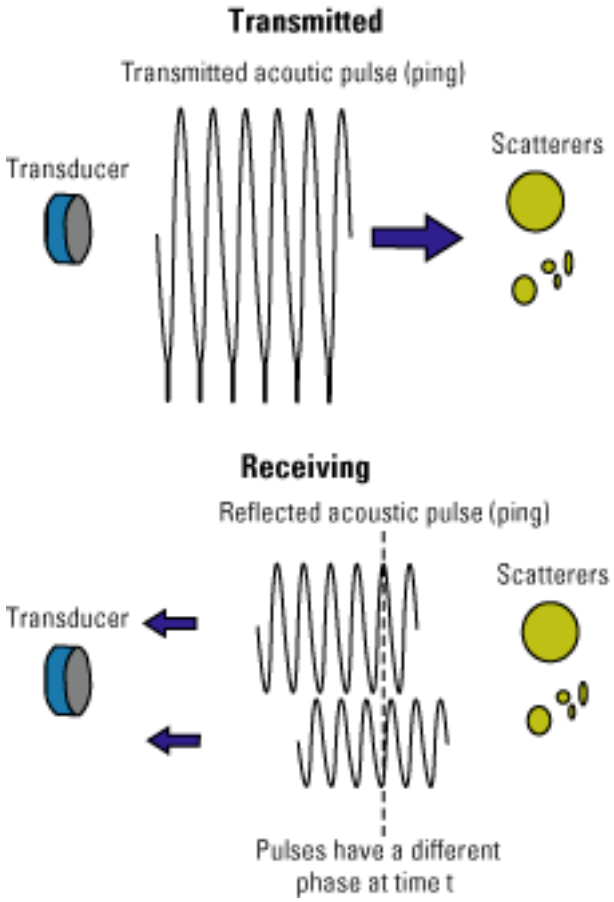


**Figure 1.19.** Phase change due to size and speed differences of scatterers.

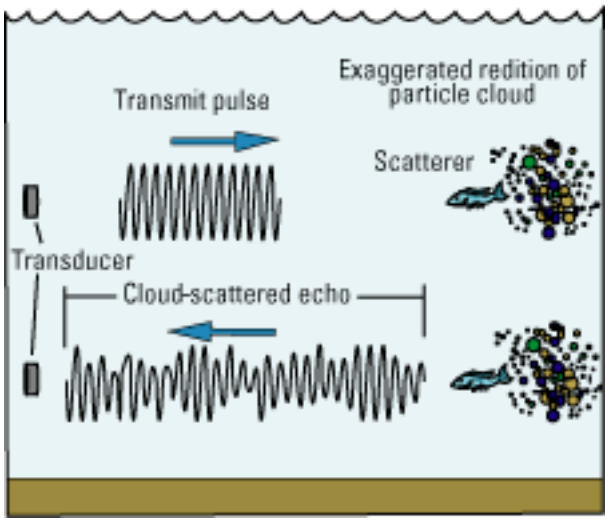


**Figure 1.20.** Echo returned from a cloud of particles.

orders of magnitude; therefore, it is converted to decibels. The echo amplitude is a function of several things:

- Transmit pulse power
- Transmit pulse length
- Reflective quality of scatterers
- Quantity of scatterers
- Absorption coefficient of the water

When the echo amplitude is high, the signal-to-noise ratio of the returned echo is high. However, when the echo amplitude drops below a certain level, the signal-to-noise ratio drops, increasing the spectral width, which, in turn, increases the uncertainty of the velocity measurement. This effect increases with range because the echo signal-to-noise ratio decreases with range. The signal-to-noise ratio also can decrease if there are too few particles in the water column. Ironically if there are too many particles (as with a very high sediment concentration), signal-to-noise ratio, from the far bin, echoes can be reduced because of absorption, beam spreading, and attenuation.

#### Side-Lobe Interference

Most transducers that are developed using present technology have parasitic side lobes that are emitted 30–40º off the main beam acoustic beam. Side-lobe interference is caused when the parasitic side lobe of an acoustic beam strikes the bottom before the main beam finishes traversing the total depth (fig. 1.21).

When the side lobe strikes the bottom, it usually swamps the receivers with an increased amplitude signal that smears the velocity information that is being gathered from the main-beam echo. On a 1,200-kHz BB-ADCP system, the loss of vertical profiling range because of this effect is approximately 15 percent with 30º-beam angles and 6 percent with 20º-beam angles.

Figure 1.22 shows a screen shot of a typical Doppler profile showing the backscattered amplitude or, using an RDI-coined term, the “reflected signal

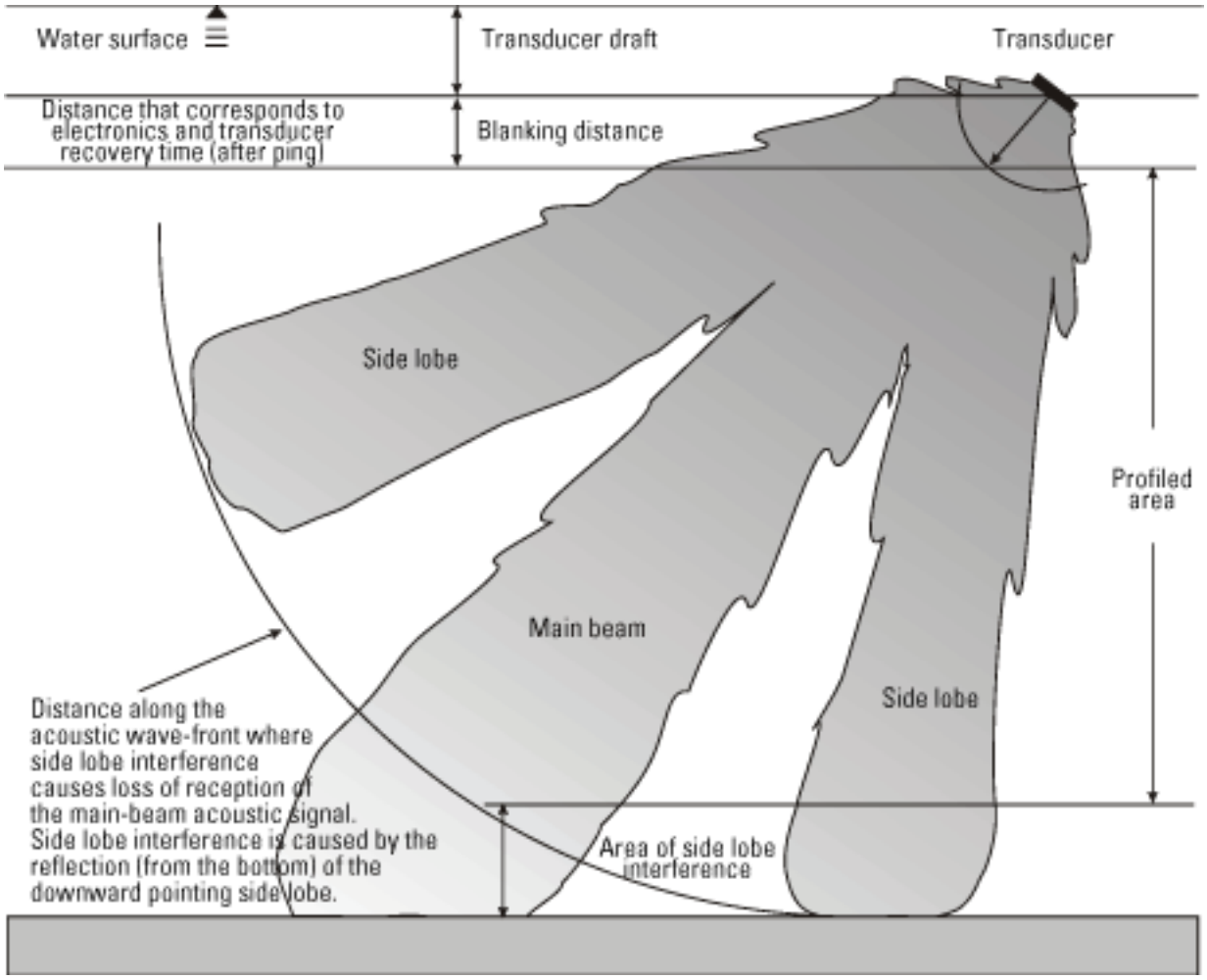


**Figure 1.21.** Acoustic Doppler current profiler transducer beam pattern.

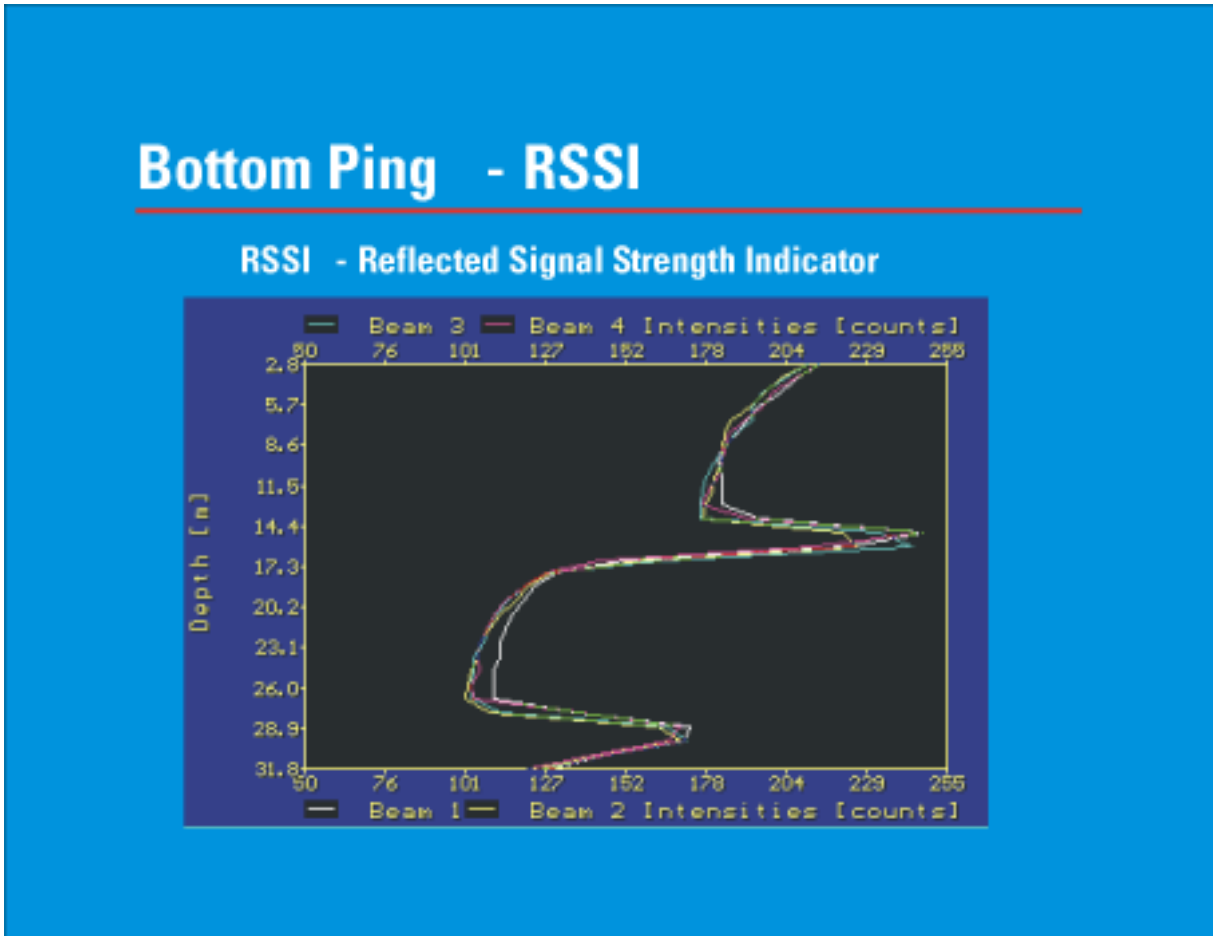


**Figure 1.22.** Reflected signal strength indicators (RSSI) for a four-beam acoustic Doppler current profiler.

strength indicator" (RSSI). Notice that the RSSI falls off logarithmically with depth until the side lobes strike the bottom. A sharp increase in the RSSI occurs when the side lobes hit the bottom because the bottom is such a strong reflector. Another reflection is seen below the first bottom reflection. This is called a multiple, and it occurs when the signal is reflected off the bottom, travels to the surface, and is reflected off the surface. Note that the multiple is twice the depth as the "original" bottom echo.

#### Effects of Different Beam Angles

Although using smaller beam angles increases the percentage of the profile that is measured, the precision of water-velocity measurements also is reduced because of decreased coupling with the horizontal. The formula for this calculation is shown in equation 1.4 (R.D. Instruments, Inc., 1989):

$$R_m = D\cos(A) \qquad (1.4)$$

where

$R_m$ = maximum measurable range, in meters;

$D$ = distance from the ADCP to the channel bottom, in meters; and

$A$ = angle of the beam relative to the vertical, in degrees.

The standard deviation of single-ping water-velocity measurements decreases as a function of beam-pointing angle (angle between beam and the vertical). If standard-deviation values are known for a given beam angle, they can be predicted for other beam angles using the ratio of the sines of the angles (eq. 1.5).

$$\sigma_u = \frac{\sigma_a \sin(A)}{\sin(a)} \qquad (1.5)$$

where

$\sigma_u$ = predicted single ping standard deviation of measured horizontal water velocity, in centimeters per second;

$\sigma_a$ = single-ping standard deviation of measured horizontal water velocity, in centimeters per second, using beam angle *a*;

*A* = beam angle *a*, in degrees; and

*a* = beam angle of predicted measurement, in degrees.

Note that $\sigma_u$ approaches infinity as the beam angle approaches zero (fig. 1.9).

#### Blanking Distance

After transmitting acoustic pulses, the transducers and associated electronics must rest a short time before receiving the reflected acoustic signals. A good analogy of this effect is a large gong. The vibrations from a gong take a long time to die out (sometimes several minutes). A transducer ceramic is similar to a miniature gong in that the pulse (ping) vibrations at the 1,200-kHz resonant frequency must be allowed to die out before the transducer is used as a listening device. These tiny vibrations last about 170 microseconds. During that time, the acoustic pulse has traveled about 0.3 m (0.98 ft) if sound velocity is assumed to be 1,500 meters per second (m/s) [4,921 feet per second (ft/s)], and velocity measurements cannot be made within that distance (fig. 1.21).

The actual distance to the first measured bin depends on several factors:

- Blanking distance
- Speed of sound
- Operating mode
- Bin size
- Transmit frequency
- Transducer beam angles

## Instrument Development: Solving the Problem of Velocity-Measurement Uncertainty

Aside from the instrument errors discussed in the previous section, most early ADCP measurement systems suffered from "sloppiness," or in more technical terms, "velocity-measurement uncertainty." Single-ping velocity uncertainty for an RDI narrow-band 1,200-kHz ADCP purchased in 1986 (using default settings), for example, was 13 cm/s (0.43 ft/s). Luckily this "sloppiness" is, for the most part, random and can be reduced by data averaging. "Narrow-band" is defined later in this chapter. The following section discusses the reasons for velocity-measurement uncertainty and some techniques used to reduce it.

#### Random and Bias Error

When using an ADCP, two types of errors contribute to velocity uncertainty; random error and bias. Bias errors are sometimes called systematic errors. Random error can be reduced by data averaging; bias error cannot. A thorough understanding of these two types of errors is a crucial prerequisite to the assessment of ADCP velocity and discharge measurement accuracy.

#### Random Error

ADCP sources of random error are as follows:

- Pulse length—The shorter the pulse length for a given frequency in a narrow-band ADCP, the greater the random error
- Transmit frequency—the lower the frequency at a given pulse length (or lag distance), the greater the random error
- Signal-to-noise ratio—the lower the signal-to-noise ratio, the greater the random error
- Beam angle—As the beam angle approaches vertical, random error approaches infinity

A random velocity-vector error is composed of a random magnitude and a random direction. Figure 1.23 shows 1,920 pings (individual velocity measurements) taken on a lake near Sacramento, California, using a BB-ADCP. Velocities were taken in still water from depth cell number 10 (bin 10) and averaged into 10 ping groups that gave a total of 192 velocity averages. The north and east components were averaged for 10 pings each and the resultant averages were converted to polar coordinates, then plotted. Notice that the error pattern is similar to the pattern of a shotgun blast, with the errors evenly distributed around zero. A directional bias would show as a nonuniform pattern of data points distributed along one of the directional axes.

Random error is reduced by the square root of the number of samples. When data averaging reduces random error magnitudes below the value of bias errors, further averaging becomes superfluous. Figure 1.24 shows the same set of data as in figure 1.23 averaged for about 200 pings; the same set of data yields nine averages.

#### Bias Error

A velocity-vector bias has a fixed magnitude and direction that either is constant or proportional to the measured velocity. Bias error is nonrandom and, therefore, cannot be reduced by data averaging. Fortunately, in most cases, bias error in ADCP-measured velocities and discharge measurements is

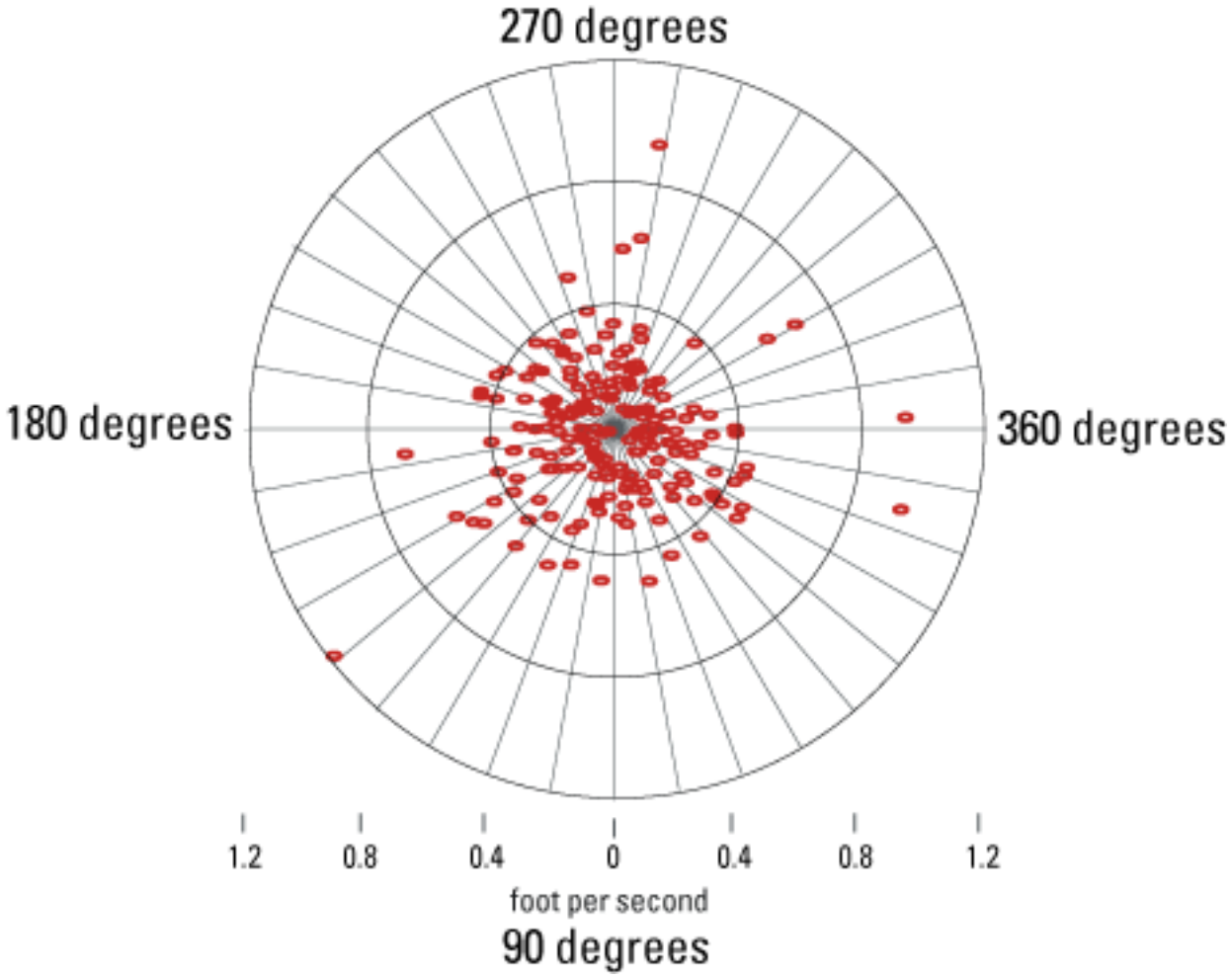


**Figure 1.23.** Polar plot of 10-ping broad-band acoustic Doppler current profiler velocity averages.

small. Examining figure 1.24 reveals that there may be a small bias error or an actual water velocity in the lake at a direction of 250º. Random and bias error are discussed in more detail in this report in the sections on velocity and discharge-measurement errors.

### Pitch and Roll

Pitch is defined as rotation along the fore/aft axis of the ADCP, whereas roll is defined as rotation in the direction of the starboard/port axis of the ADCP. Most ADCP systems contain instruments that detect the magnitude of pitch and roll, as well as methods to correct ADCP-measured velocities for the effects of pitch and roll. Figure 1.25 shows the pitch and roll axes as they apply to a boat-mounted ADCP.

Corrections for pitch and roll of an ADCP must address velocity corrections and depth corrections. The velocity corrections are needed because the geometry of the beam angles change, with regard to the flow field (eq. 1.3, fig. 1.8), during instances of pitch and roll.

Changes in bin depths also are evident during pitch and roll occurrences (fig. 1.26). Bottom depths and bin depths must be “remapped” during an ADCP pitch and roll occurrence. For small angles of pitch and roll, these corrections are not significant unless velocity profiles in all three orthogonal coordinates are desired. Values of horizontal water velocity are a function of the cosine of the pitch and roll, which is insignificant for angles less than 5º. However, if accurate vertical velocities are desired, even small amounts of pitch and roll can significantly affect accuracies. ADCPs commonly are designed with pendulum-type pitch and roll sensors, which are affected by acceleration. However, if an ADCP is expected to be used primarily aboard a vessel in areas having large waves, then fast-responding gyroscope systems should be used to compensate for pitch and roll.

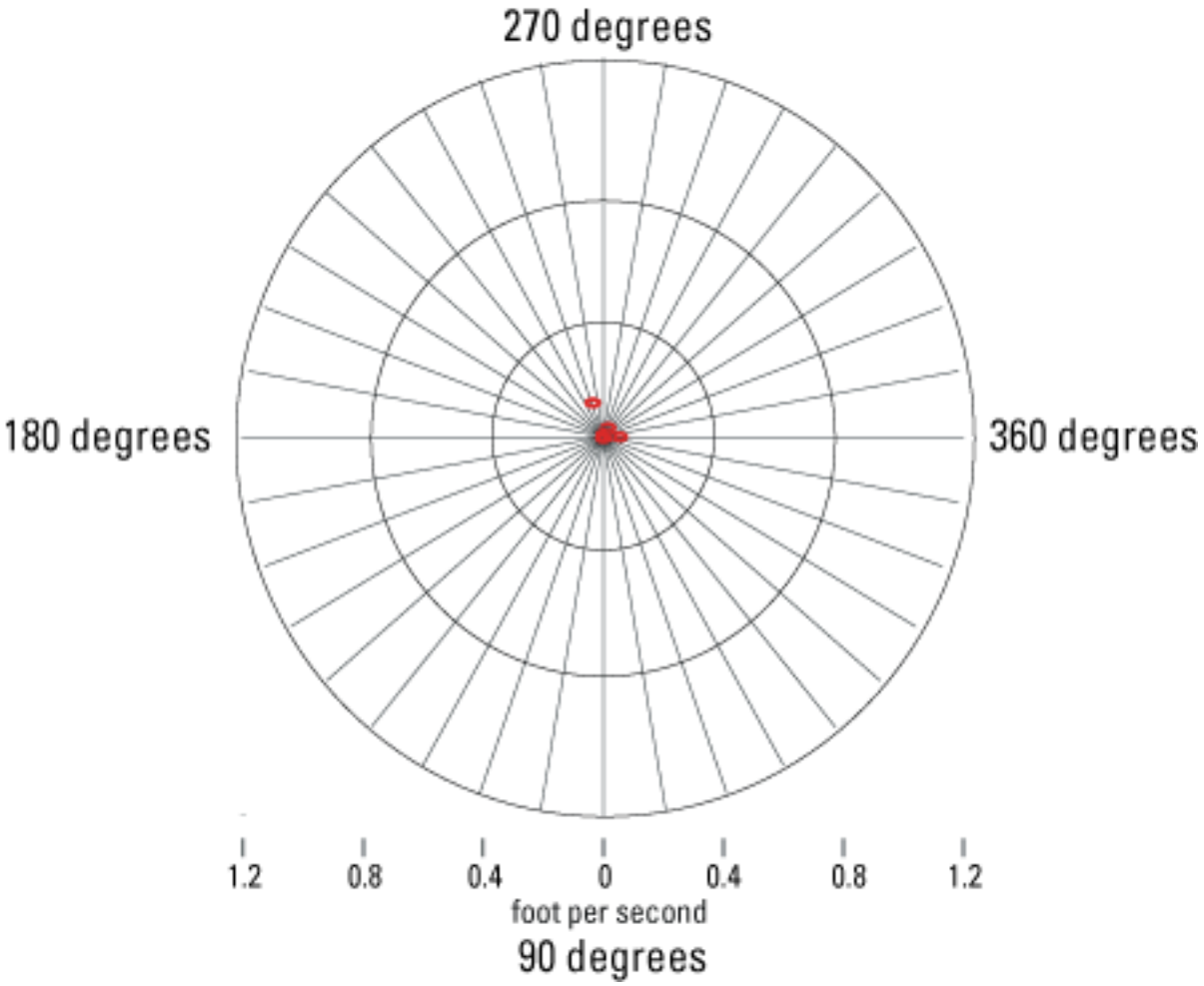


**Figure 1.24.** Polar plot of about 200-ping broad-band acoustic Doppler current profiler velocity averages.

### Beam-Angle Error

Errors in the beam angles could have been a significant source of bias error with early ADCP systems before the manufacturer instituted quality-assurance procedures to minimize this type of error. Beam-angle errors are best detected on a fixed distance course. The manufacturer has developed a computer program that accurately calculates ADCP beam-angle errors, based on data that are collected on the fixed distance, lake, or bay course. Beam-angle errors also will show as biases during intercomparison tests with conventional discharge measurements or other discharge-measurement devices.

Beam-angle errors can be eliminated in recently developed (after 1993) ADCP firmware by introducing corrections into the ADCP system flash memory. This procedure should be done only by the manufacturer. Suspect systems should be sent to the manufacturer for beam-angle testing and recalibration.

### Narrow-Band and Broad-Band Doppler Shift Measurements

"Narrow band" is not a very descriptive term and is used here only because the term is used in the industry to describe a certain type of ADCP instrument. The term is used to describe a pulse-to-pulse incoherent ADCP. This means that in a narrow-band ADCP, only one pulse is transmitted into the water, per beam per measurement (ping), and the resolution of Doppler shift must take place during the duration of the received pulse. In the case of RDI-manufactured narrow-band ADCPs, this is accomplished using an autocorrelation technique.

The broad-band (BB) ADCP was developed by RDI in an attempt to solve some of the measurement uncertainty problems seen with the narrow-band ADCP. In a BB-ADCP, the Doppler shift is resolved by transmitting two pulses of the same shape that are in phase with each other (pulse-to-pulse coherent). The following section describes, in detail, the operation of narrow-band ADCPs and BB-ADCPs.

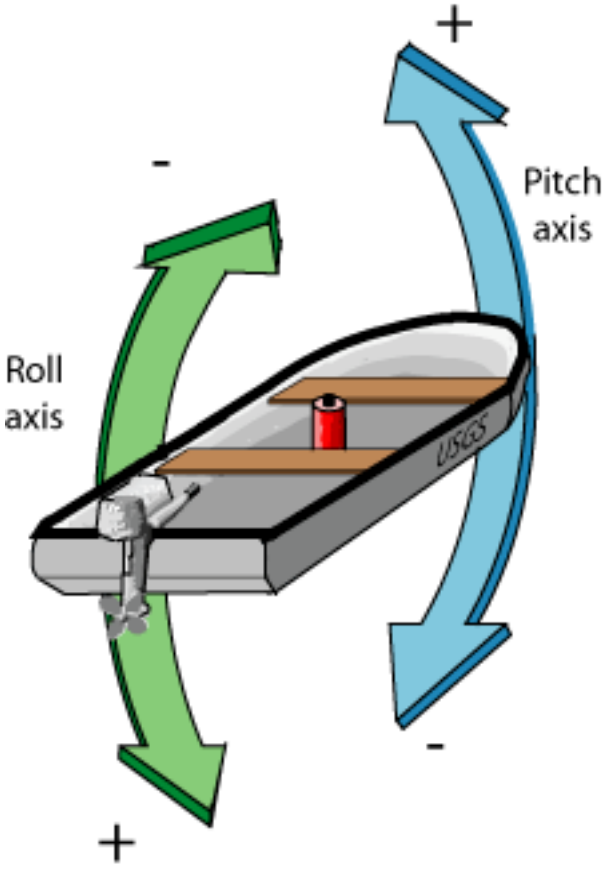


**Figure 1.25.** Pitch and roll axes for a boat-mounted acoustic Doppler current profiler.

### Narrow-Band Doppler Shift Measurements

Doppler shift can be described as the perceived frequency shift of a transmitted (and then reflected) signal caused by the movement of the reflector. Doppler effect also can be described as the magnitude of the phase difference between two coherent (but independent) samples of a reflected signal. The following analogy provides an explanation of narrow-band Doppler shift velocity measurements.

Joel Gast (R.D. Instruments, Inc., oral commun., 1992) has likened a narrow-band Doppler shift measurement to the measurement of automobile speed on a freeway (at night) using a strobe light and a high-speed camera. Consider a freeway at night with traffic moving at a steady rate of speed. A camera has been placed near the freeway and posts have been installed at set distances within the camera's field of view. A strobe light is actuated and, while the freeway is illuminated by the single-strobe pulse, the camera takes two high-speed photographs. When the investigator examines the photographic negatives he finds that by lining up (synchronizing) the images of the cars on the two photographic negatives, the distance traveled by the cars can be determined by measuring the apparent shift in position of the reference posts (fig. 1.27). The auto speeds also can be calculated by multiplying intrapost distance by the lag time between the two photos. If the strobe flashes become acoustic pulses, the cars become reflective particles in the water column, and the negatives become the received

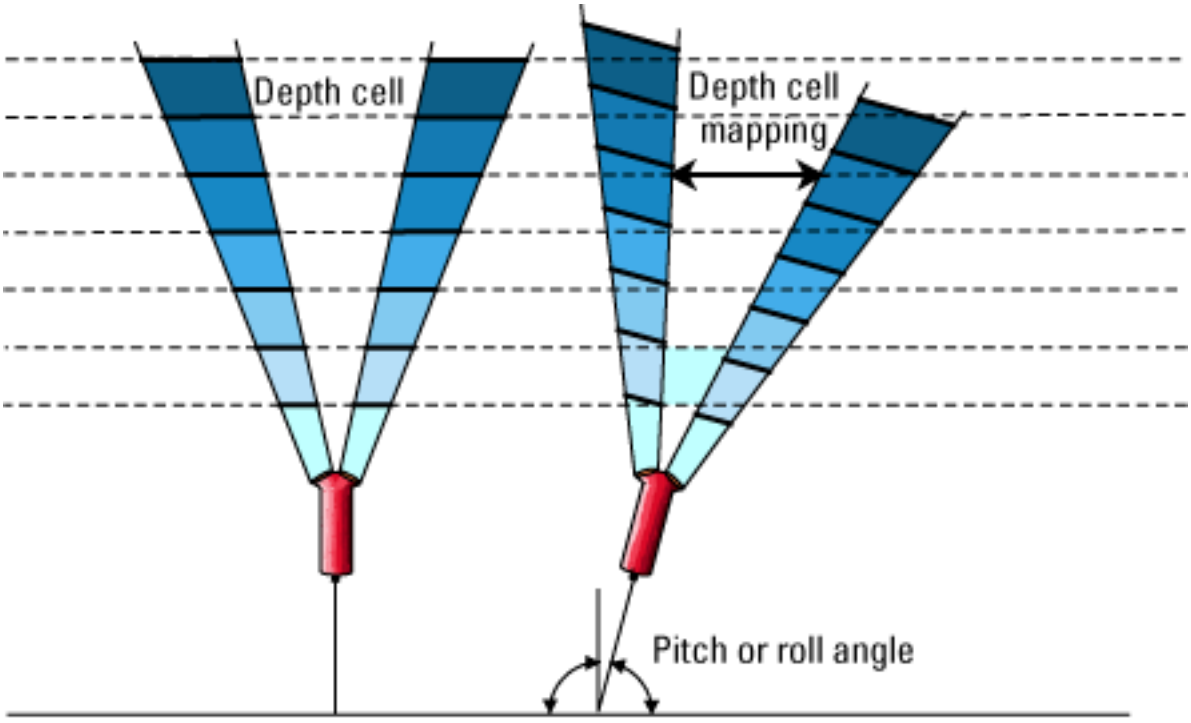


**Figure 1.26.** Bin positions during an acoustic Doppler current profiler roll occurrence.

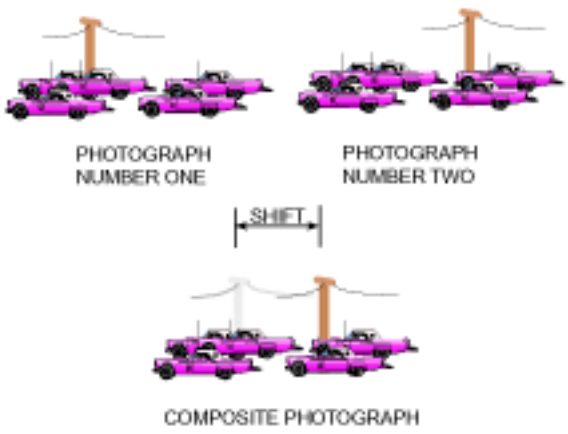


**Figure 1.27.** Freeway strobe-light system used to measure vehicle speed.

reflected signals, this scenario becomes roughly analogous to the workings of a narrow-band ADCP system.

The drawback to such a system is that the strobe pulse dissipates very quickly and the two photos must be taken while the same cars are still illuminated by the strobe. This means that time lags are very short and the distance traveled by the cars (reflectors) is very short; therefore, the car speeds cannot be measured precisely. Because of these limitations, velocity measurements made using the narrow-band technology are "noisy" (have a relatively high random error). Figure 1.28 shows a diagram of a narrow-band Doppler shift measurement. The signal is sampled twice during the reception of the reflected signal. The lag-time between

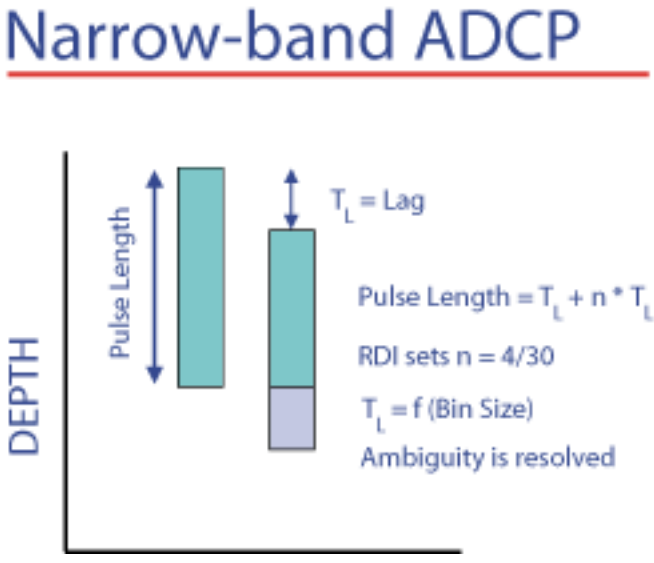


**Figure 1.28.** Narrow-band acoustic Doppler current profiler (ADCP) shift measurement. RDI, R.D. Instruments, Inc.

each measurements is shown as $T_L$. Using an auto-correlation technique, the Doppler shift is then calculated. In the narrow-band ADCP, the pulse length depends on the lag ($T_L$) which is a function of bin size. A filter scheme that looks at the whole returned signal is used to resolve ambiguity.

#### Broad-Band Doppler Shift Measurements

Using the freeway analogy, if the investigator decides to install another camera a distance of ten or more car lengths (parallel to the freeway) from the first camera, he could actuate a strobe, take a picture with the first camera, wait a short time, actuate another strobe, then take a picture with the second camera. If the strobes are timed correctly, the cars will travel from the field of view of the first camera into the field of view of the second camera during the time between photos. The investigator synchronizes the positions of the cars on the two negatives and finds that there is a much longer lag time (time between each strobe versus the time between two photos taken during the same strobe) and that the cars traveled a longer distance. The investigator then can calculate the speed of the cars with much greater precision than with the single-strobe system. The distance between the cameras and the time between each strobe must be chosen carefully. If the investigator waits too long between strobes, random movement between the cars (passing, slowing down, speeding up, and so forth) will render the two negatives "unmatchable" (uncorrelated). Transmitting a pair of pulses (strobes) into the water allows for much longer lag times (therefore, more precision) than the narrow-band system. The investigator finds, however, that there are some "costs" associated with this technique.

One of the most significant costs is self noise. The description of self noise again uses the freeway analogy. Suppose that, because of limitations in photographic technology, the freeway cameras have no shutters. Because the investigator must leave the camera shutters open, both cameras will "see" the traffic illuminated by the two strobes. However, only 50 percent of the "scenery" will be usable to both cameras for correlation purposes. For example, the film in camera one is exposed once during the first strobe. The cars then travel out of the field of view of camera one and into the field of view of camera two. However, the film in camera two already has been exposed by the flash of the first strobe and, thus, any cars photographed have left the field of vision. When the second strobe flashes, the film in both cameras is again exposed (double exposed) and the cars that were first photographed by camera one are now photographed by camera two. Because the film has been double exposed, only 50 percent of the scenery in each exposure contains cars that are common to both cameras.

As in the film of the freeway cameras, the reflected wave front from the first BB-ADCP pulse-pair is again "exposed" by the incident wave front of the second pulse and, therefore, is subject to the same "double exposure." The increased noise due to this 50-percent correlation is reduced by data averaging (very narrow pulses can be used, and, therefore, large amounts of data can be collected and averaged). Without a technique called phase coding (discussed later in this section) and a high signal-processing rate, BB-ADCP velocity measurements would be less precise (because of self noise) than measurements made by the narrow-band ADCP system.

The BB-ADCP cannot only measure the phase angle differences between pulse pairs, but can measure the change in lag spacing between transmitted and received pulse pairs (time dilation). This pulse-pair measurement concept can be visualized using a series of illustrations depicting a stationary particle, a moving particle, and the effects of these particles on lag times between reflected pulse pairs in a liquid medium. Figure 1.29 shows a transmitted pulse pair from a stationary source approaching a stationary particle.

Figure 1.30 shows the same pulse pair reflected from a stationary particle. In the case of a stationary particle, lag A (fig. 1.29) is equal to lag B (fig. 1.30). Now assume that the particle is moving away from the transducer. Figure 1.31 shows the aforementioned transmitted pulse pair approaching a moving particle. Figure 1.32 shows the pulse pair after their reflection from the moving particle.

Note that, in the case of a moving particle, the reflected pulse lag distance (lag B) has increased because the particle's movement delays the reflection of the second pulse, relative to the first. Although this

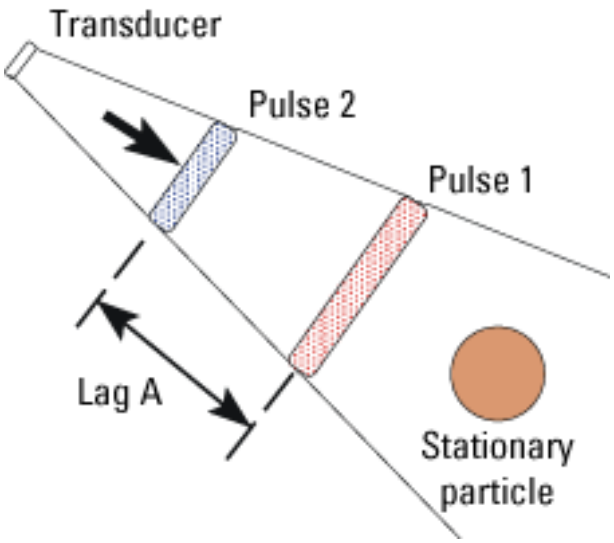


**Figure 1.29.** Acoustic pulse pair approaching a stationary particle.

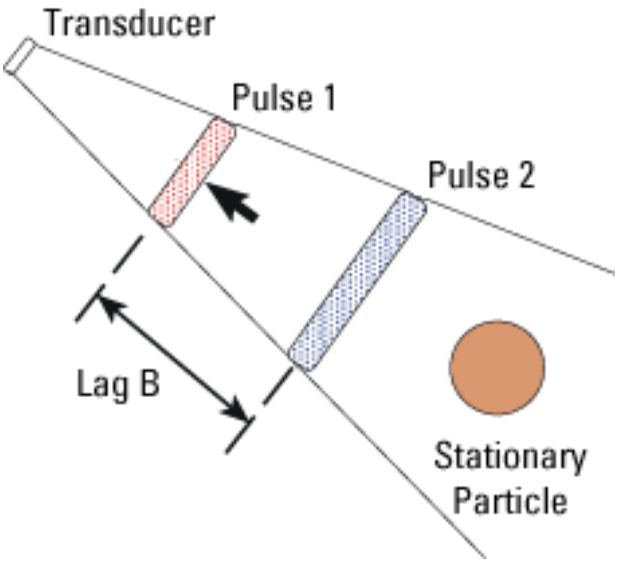


**Figure 1.30.** Acoustic pulse pair reflected from a stationary particle.

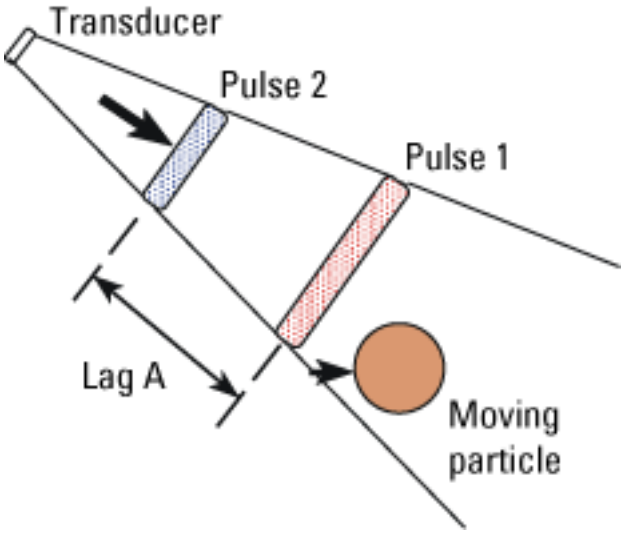


**Figure 1.31.** Acoustic pulse pair approaching a moving particle.

can be thought of as a time-domain phenomena, it is really a description of Doppler effect. The transmitted pulse repetition frequencies appear to vary in accordance with changes in the speed and direction of the transducer and (or) reflector.

Lag distance between the reflected pulses increases as the transducer and particle move apart. The opposite occurs if the particle and transducer move together. The difference between transmitted and received lag distance is proportional to the speed of the particle (relative to the transducer) or the transducer (relative to the particle). The difference in lag distance is exaggerated in these examples to aid comprehension. In reality, the ratio of the sound speed in water

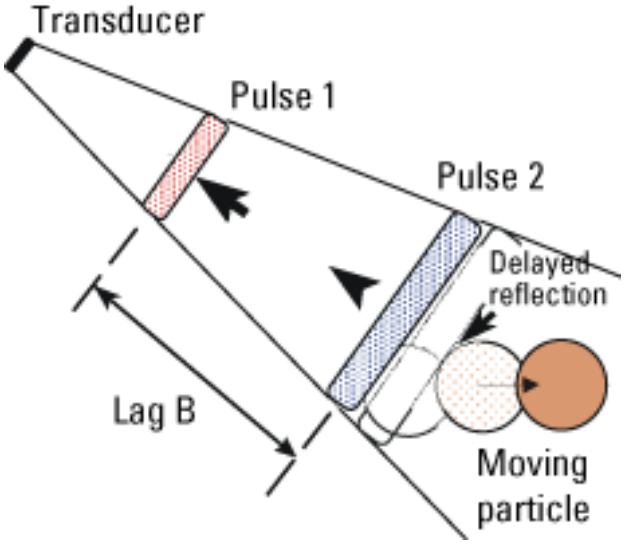


**Figure 1.32.** Acoustic pulse pair reflected from a moving particle.

[1,500 m/s (4,921 ft/s)] to the particle speed [0–2 m/s (0–6.6 ft/s)] results in very small lag differences. If a particle is moving slowly, the lag differences will be small and hard to measure. For that reason, discharge measurements of flows with low water velocities (0.05 m/s or less) are imprecise using the BB-ADCP discharge-measurement system unless special methods are employed. The accurate measurement of these lag differences is discussed in the next section.

Self noise can be visualized as shown in figure 1.33. When pulse "a" illuminates an object, a small pressure wave is reflected back toward the transducer. This pressure wave contains pure information about the speed of the object that caused the reflection. The passage of pulse "b" through the reflected pressure wave again illuminates scatterers in the vicinity of the pressure wave and contaminates the pure speed information of the pressure wave with unwanted noise. This contamination causes a dramatic increase in the single-ping random error of the velocity determination.

Another cost for using the increased lag spacing available with the BB-ADCP system is velocity ambiguity. The freeway analogy is not appropriate to explain the velocity ambiguity phenomenon, therefore, a circular racetrack analogy is used (figs. 1.34a, b). Suppose the investigator decides to mount cameras and strobe systems in a helicopter that hovers above a circular racetrack at night. Both cameras are mounted so that the racetrack is within their field of view. The circumference of the racetrack has been estimated and some reference poles (visible around the edge of the track) have been identified. The investigator tests the strobe and finds that just the outlines of the cars can be

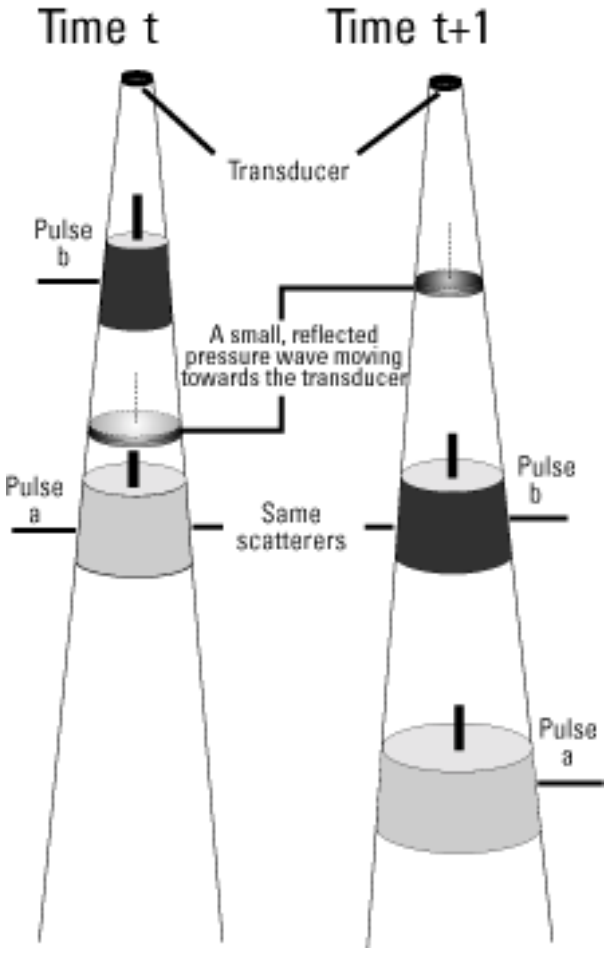


**Figure 1.33.** Acoustic pulse pair with a small reflected pressure wave.

seen. The camera shutter is opened, and the first of two strobe flashes is actuated. After a short time, the other flash is actuated. The investigator rotates the developed negatives to synchronize the car outlines and estimates their speed by multiplying the distance between the poles by the time between strobe flashes.

This speed-measurement system works well until the car speeds increase substantially or the investigator decides to increase the time between strobe flashes (lag times) to improve measurement precision. After the first strobe flash, the cars complete one lap (past the spot where they were first photographed) before the second strobe flash. When the investigator attempts to synchronize the negatives, he becomes confused because he cannot determine how many (if any) laps the cars have completed or whether the cars have gone forward or backward.

The "ambiguity velocity" is the velocity the cars must achieve before this confusing circumstance happens. If the strobe flashes are temporally close, the ambiguity velocity is high (higher than the cars

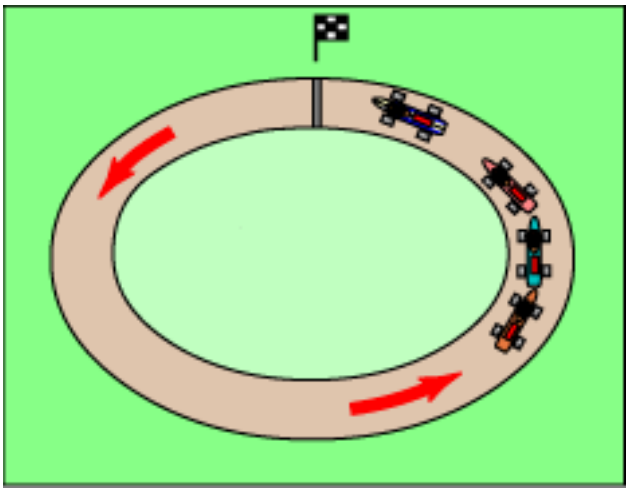

**Figure 1.34a.** Race track analogy during the first strobe flash.

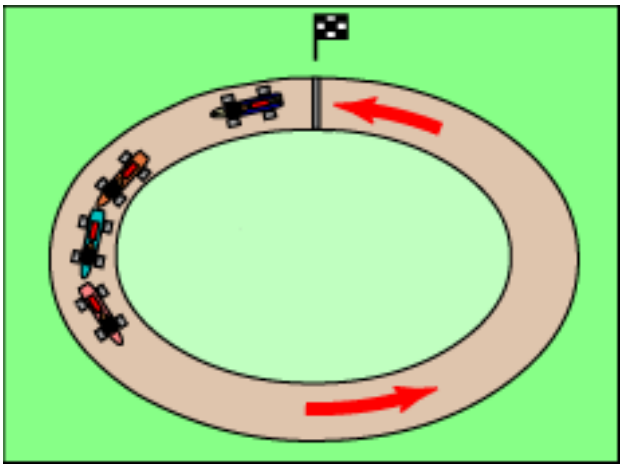

**Figure 1.34b.** Race track analogy during the second strobe flash.

normally travel) but measurement precision is lower because the cars have traveled a shorter distance between strobe flashes. If the investigator lengthens the time between strobe flashes (lag) to improve the measurement precision, the ambiguity velocity becomes lower and, therefore, more troublesome.

The primary method of measurement used by BB-ADCP systems is the measurement of phase-angle differences between the pulse pairs. This measurement is subject to ambiguity errors because the yardstick used to make these measurements actually is one-half of one cycle at the transmitted frequency. Figure 1.35 shows the error factor when the speed of the measured velocity exceeds the ambiguity velocity. The colored circle represents one cycle of transmitted energy with a possible phase measurement capability of 0–360º. In this example, we will let 1 millimeter per second (mm/s) equal 1º of phase change. We have no trouble measuring plus and minus 10 mm/s or even plus and minus 170 mm/s using our one-half cycle yardstick, but when the measured velocity is 190 mm/s, our yardstick reads a velocity of –170 mm/s. This is an error of 360 mm/s. Notice that this ambiguity velocity is 180 mm/s and is equivalent to 180º on our circular yardstick. The measurement error (when the ambiguity velocity is exceeded) is always equal to two times the ambiguity velocity.

The BB-ADCP (and even the narrow-band ADCP) may report an erroneous velocity caused by ambiguity when scatterer velocities are high enough that their movement between lags exceeds one-half of the transmitted frequency wavelength. Because a 1,200-kHz BB-ADCP uses the change in phase of a 1,200-kHz sinusoid for a Doppler shift "ruler," it is impossible to identify which cycle of the reference signal to use when calculating the phase shift between the two returned reflections when the reflected signal phase shift is greater than one-half of one wave length. To solve this problem, the manufacturer has included a signal processing technique that corrects for ambiguity errors. This technique takes additional time, however, and somewhat slows the water ping rate. Shortening the lag distance increases the ambiguity velocity, causing it to be more noticeable and less bothersome, especially if water and bottom velocities are significantly lower than the ambiguity velocity. However, decreasing the lag distance also increases noise (standard deviation of measured velocities).

The ambiguity velocity of a 1,200-kHz BB-ADCP can be estimated by equation 1.6 (L.Gordon, R.D. Instruments, Inc., written commun., 1992):

$$U_a = \frac{47}{L} \qquad (1.6)$$

where

$U_a$ = the ambiguity velocity, in meters per second; and

$L$ = the lag specified by the BB-ADCP "&L" command.

The maximum allowed ambiguity velocity is 5.2 m/s (17 ft/s) ($L$ = 9) for a 1,200-kHz system. Contamination of the measured data shows up as velocity spikes at the ambiguity interval (twice the ambiguity velocity). This means that if ambiguity errors are suspected, the (unaveraged) data should be examined for velocity spikes of the opposite sign that, when compared with the last good measured velocity, have a difference of about twice the ambiguity velocity.

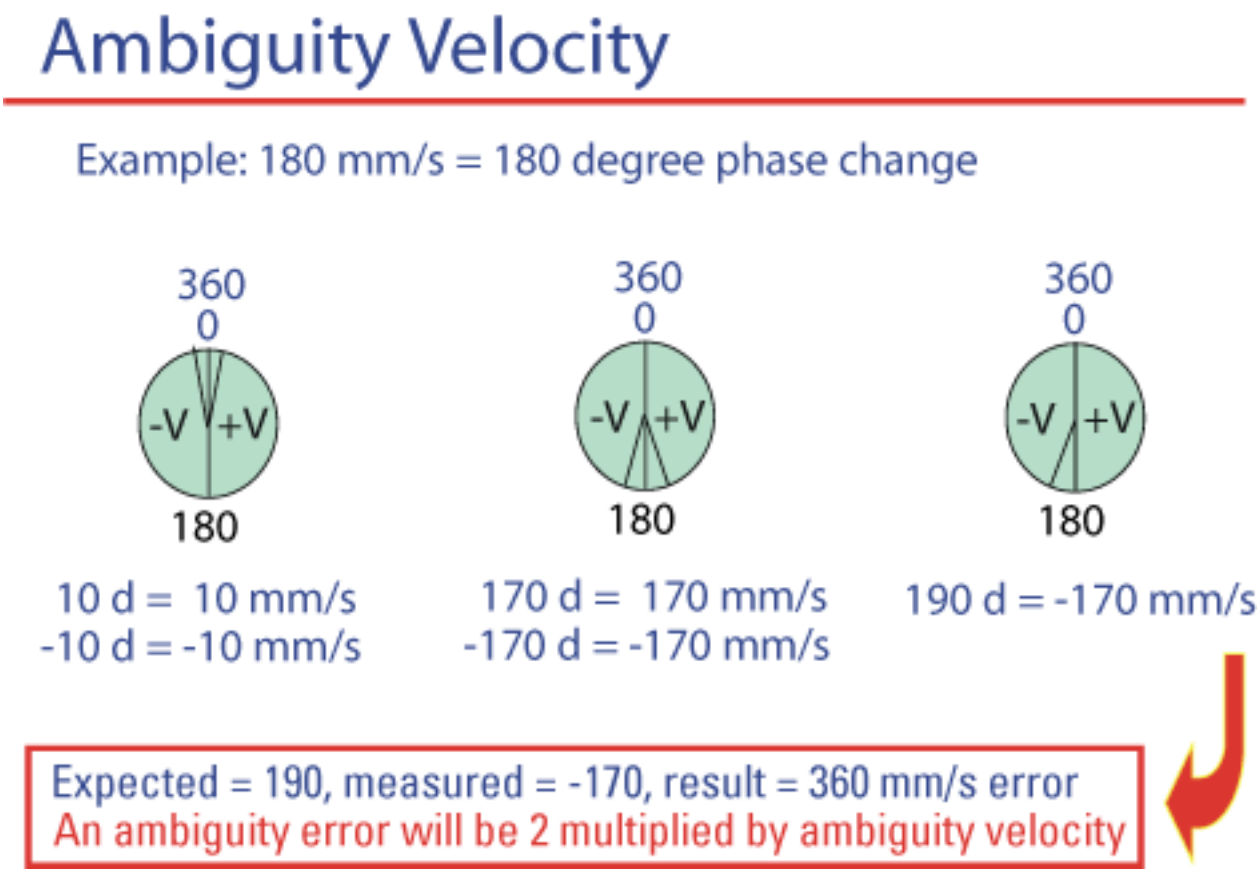


**Figure 1.35.** Explanation of ambiguity velocity. mm/s, millimeter per second; V, velocity; d, degree.

#### Differences Between Phase-Shift Measurements and Lag-Spacing Measurements (Time Dilation)

An unambiguous measurement can be obtained from the returned Doppler information by looking at the change in lag spacing (figs. 1.31, 1.32) but this method of measuring time dilation is much less precise than the measurement of phase-angle difference. Figure 1.36 shows the differences between phase angle and time dilation. Note that even though the ambiguity velocity has been exceeded in the last example, the time-dilation measurement still provides a "ball-park" measurement of velocity. The time-dilation method usually is used to resolve ambiguities.

#### Bottom-Tracking Limitations

To measure discharge, the ADCP must sense and measure the velocity of the ADCP, relative to the river bottom (bottom tracking). If the velocity of the water is known, relative to the ADCP, and the velocity of the ADCP is known, relative to the river bottom, then the water velocity, relative to the bottom, can be calculated. The bottom-track pulse must be somewhat longer than the water-track pulse to properly illuminate the bottom (fig. 1.17). In many cases, a group of water-velocity pings is averaged along with one or more bottom-track pings to form an averaged ensemble. To compute discharge, the ADCP must provide the horizontal water and boat velocity components, depth, and time between ensembles. The ADCP discharge-measurement software discussed in chapter 2 uses these data to calculate a vector cross product at each bin and then uses an extrapolation scheme to estimate the cross products in the unmeasured areas near the top and bottom of the profile (eq. 2.2, chap. 2).

The discharge-measurement software then integrates these cross products over the profile depth to obtain a mean, depth-weighted cross product for each ensemble. The depth-weighted cross products are summed during the cross-section traverse to produce the discharge measurement (eq. 2.2, chap. 2). Bottom tracking is required by the discharge-measurement software to compute discharge. If the river bed is moving, or if the bottom-track velocities are affected by material moving near the bottom, then the cross product will be biased. This problem sometimes can be

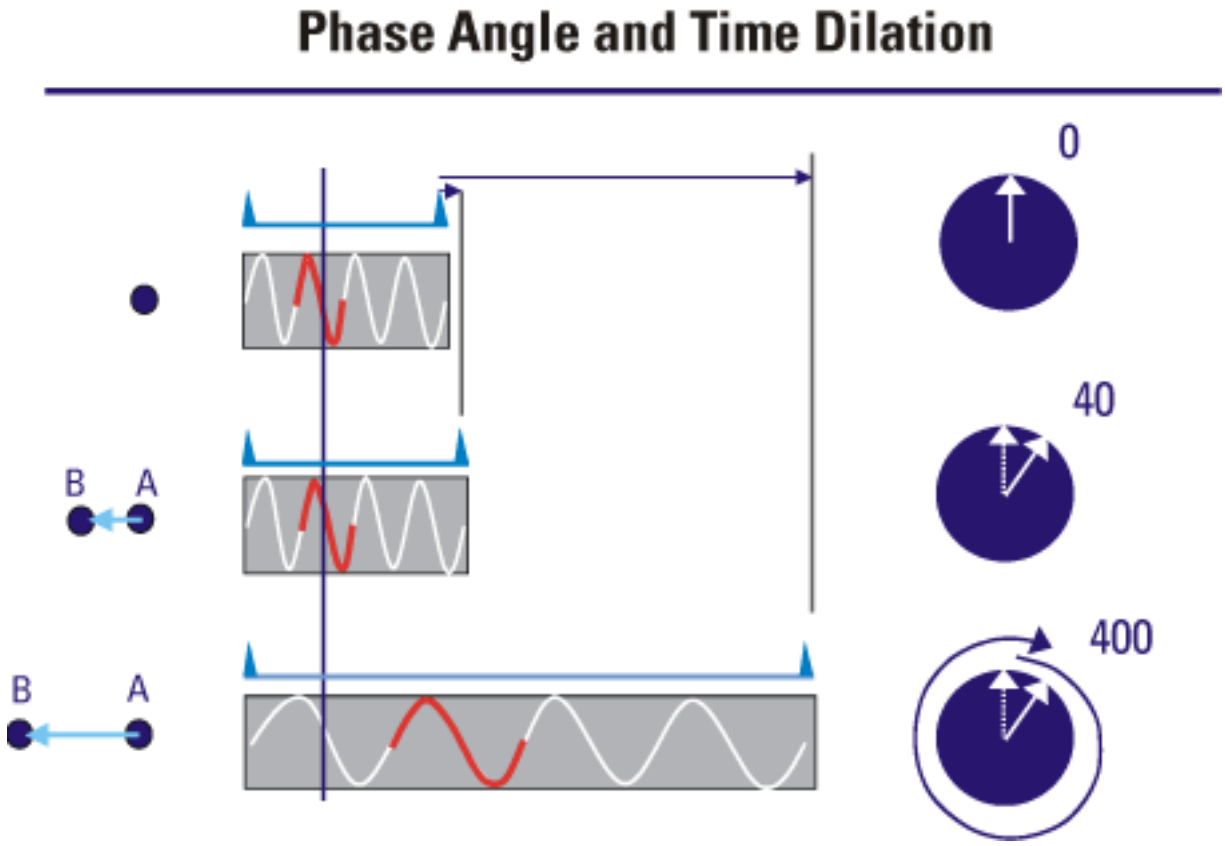


**Figure 1.36.** Description of time dilation compared with phase-angle difference.

alleviated by shortening the bottom-track pulse length (as shown in fig. 1.37) using the "&R" direct command as discussed in chapter 5. If shortening the pulse width does not work and if the river bed is moving at a speed of more than a few centimeters per minute, this bottom-track error cannot be eliminated and other means must be used to determine boat velocity (chap. 8).

## The Broad-Band Acoustic Doppler Current Profiler: Overcoming the Self-Noise Problem

### Error Sources Unique to Broad-Band Acoustic Doppler Current Profilers

In the previous section we discussed general ADCP errors. To enable a more complete understanding of the broad-band technology, we will touch upon those error sources again showing their effects on BB-ADCP systems. Although many sources of error for narrow-band ADCP systems have been discussed by Hansen (1986), Theriault (1986), Chereskin and others (1989), and Simpson and Oltmann (1993), few investigators have identified and itemized the error sources that can degrade accuracy and precision of the more recent BB-ADCP technology. Some of the known sources of error that affect the accuracy of velocity measurements (and, therefore, discharge measurements) and errors due to the physical limitations of the system are listed in this section. The signal processing technology required to accomplish water-velocity measurements with the BB-ADCP is extremely complex; the manufacturer and users will undoubtedly find new error sources during operational use of the BB-ADCP system. Major error sources in the narrow-band ADCP systems were identified over a period of 5 years (1986–91), and it is possible that the same length of time will be required to fully understand the sources of error in the BB-ADCP system, as well.

Errors that affect the performance of BB-ADCPs for velocity measurements (and, therefore, discharge measurements) can be either random or bias. As discussed earlier in this chapter, random errors can be reduced by data averaging; bias errors cannot. For purposes of this report, random errors are assumed to be Gaussian (normally distributed about the mean) and are expressed as standard deviations (in percent) of the measured mean quantity. Bias errors have sign and

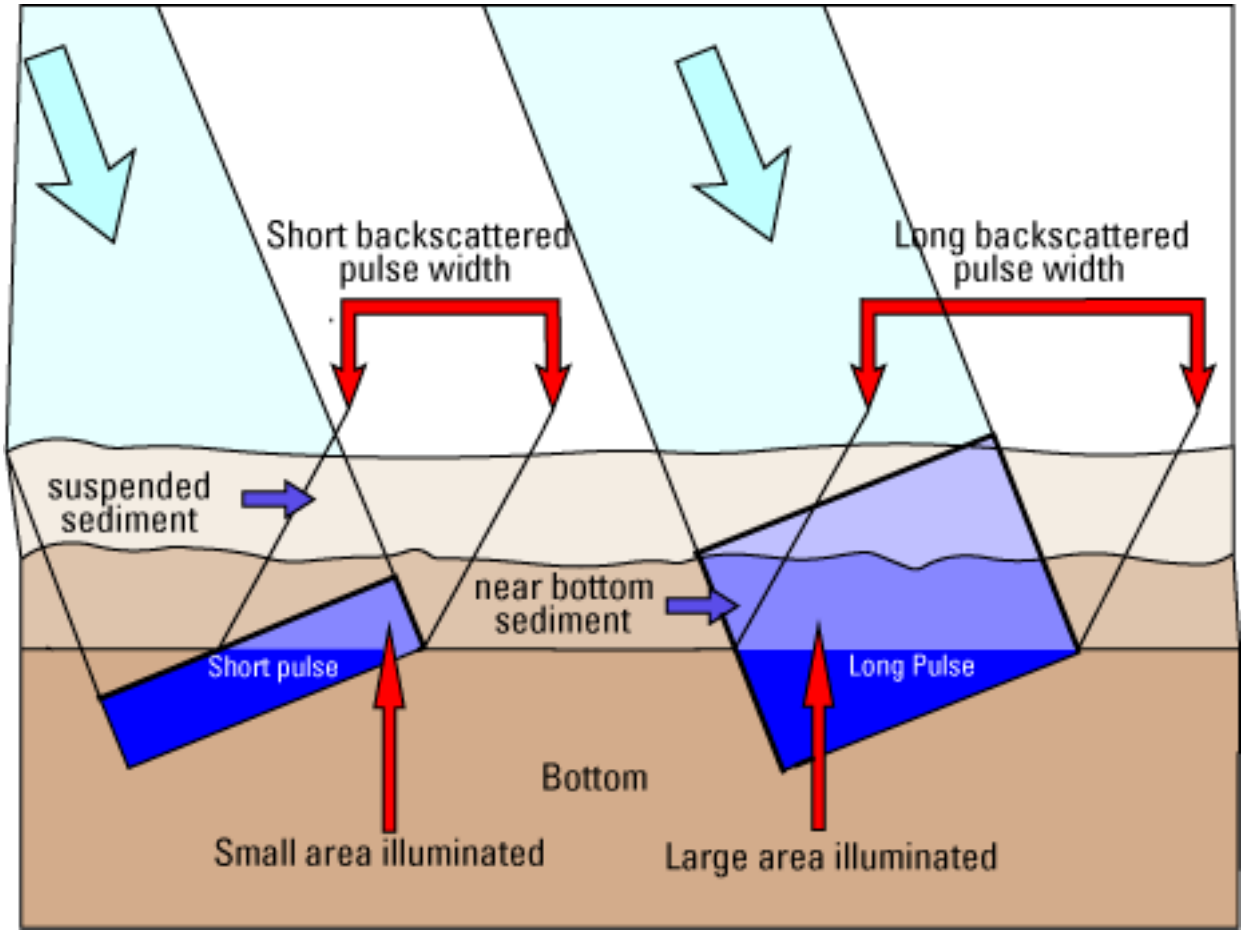


**Figure 1.37.** Effect of bottom-track pulse width on bias caused by bottom movement.

magnitude and are expressed as a percent of the "true" mean quantity, where "true" is defined as unbiased.

This report will not attempt a complete discussion of BB-ADCP bias error sources related to the physics of the acoustic signal (other than beam-angle errors and depth-measurement errors) because many of these sources are not yet documented and are beyond the scope of this report. Bias errors for the narrow-band ADCP system (with some application to the BB-ADCP system) are discussed in Simpson and Oltmann (1993). The most overwhelming source of velocity-measurement error in the BB-ADCP is random uncertainty due to self noise.

## Random Uncertainty Caused by Self Noise

Whenever a pair of pulses is used to measure water velocity (using lag times associated with the BB-ADCP), only a 50-percent correlation can be obtained from the scenery illuminated by the pulse pair when attempts are made to synchronize (autocorrelate) the reflected signals (as discussed earlier in this chapter). Figure 1.33 shows an acoustic beam with a pair of long acoustic pulses being transmitted into the water (pulse "a" and pulse "b"). Directly after the transmission of the pulse pair, the receiver begins "listening" to the pressure waves that have been reflected from scatterers in the water column. At time t, the reflected signals from scatterers in the water mass, illuminated by pulse a, begin their return path toward the transducers in the form of a small pressure wave. The small pressure wave advances toward the transducer for a short time before it is illuminated by pulse b traveling in the opposite direction. The passage of pulse b causes instantaneous reflected signals to be superimposed on the original reflected signals in the small pressure wave, creating a "double exposure." This is the 50-percent decorrelation effect caused by self noise (discussed above). The reflected signals (actually a continuum of reflected signals) travel back to the transducer. These signals are received and shunted to a delay-line register (or scratch-pad memory) for a short time while the BB-ADCP signal processor applies an autocorrelation technique to the received signals in an

attempt to synchronize (match) reflections obtained from the same water mass (data separated by the time between t and t + 1, as shown in fig. 1.33). If the lag is matched correctly, the autocorrelation function of the reflected signals will reach a peak. Because the two pulses were transmitted coherently (with the same phase), amplitude and phase information can be calculated from the function output. By using the phase information, the speed of the reflective particles can be determined, however, measurement precision is limited because of self noise.

Suppose very narrow (short) pulses are transmitted at a and b (fig. 1.38). These pulses are so narrow that 100 of them can be placed into the space occupied by the original long pulses. This modification will increase measurement precision by the square root of the number of samples (in the case of 100 samples, by a factor of 10). With this increased precision (even with the 50-percent level of self noise), the BB-ADCP capabilities surpass those of the narrow-band ADCP by almost one order of magnitude. This increased precision is gained at great cost because of the limited amount of energy the narrow pulses can deliver into the water. This energy loss caused by the narrow pulses is so great that it renders the system nearly unusable. To overcome this energy loss, the manufacturer developed a design innovation that incorporates most of the advantages of wide and narrow pulses. A wide pulse is transmitted (therefore, delivering more energy into the water than a narrow pulse), but is logically split into many small segments called code elements, each having a phase shift of either 0º or 180º (fig. 1.39).

The coding order of these phase shifts is pseudo random (behaves numerically like a random sequence). This technique has previously been applied to radar signals and some spread-spectrum communications signals (Minkoff, 1992), but the BB-ADCP manufacturer probably is the first to use this technique for water-velocity-measurement sonar.

The consequence of transmitting this phase-coded pulse-pair series into the water is that even though the pulses are long, the signal processor still must wait the full lag period (a to b) before achieving an autocorrelation peak of significant amplitude (fig. 1.40). In other words, because of the phase coding, it is difficult for the autocorrelation algorithm to realize a peak at the wrong interval.

The objective of the manufacturer is to achieve decorrelation of adjacent pulse pairs and, therefore, a

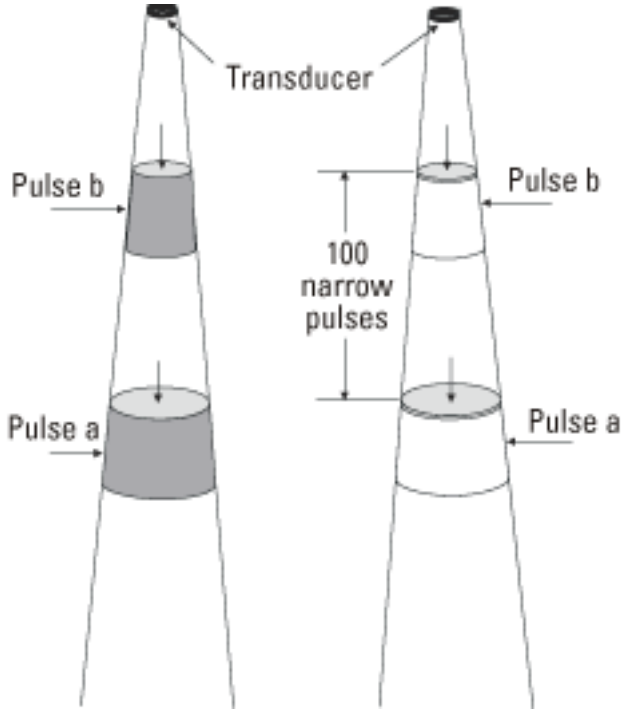


**Figure 1.38.** Narrow pulse pairs compared with wide pulse pairs.

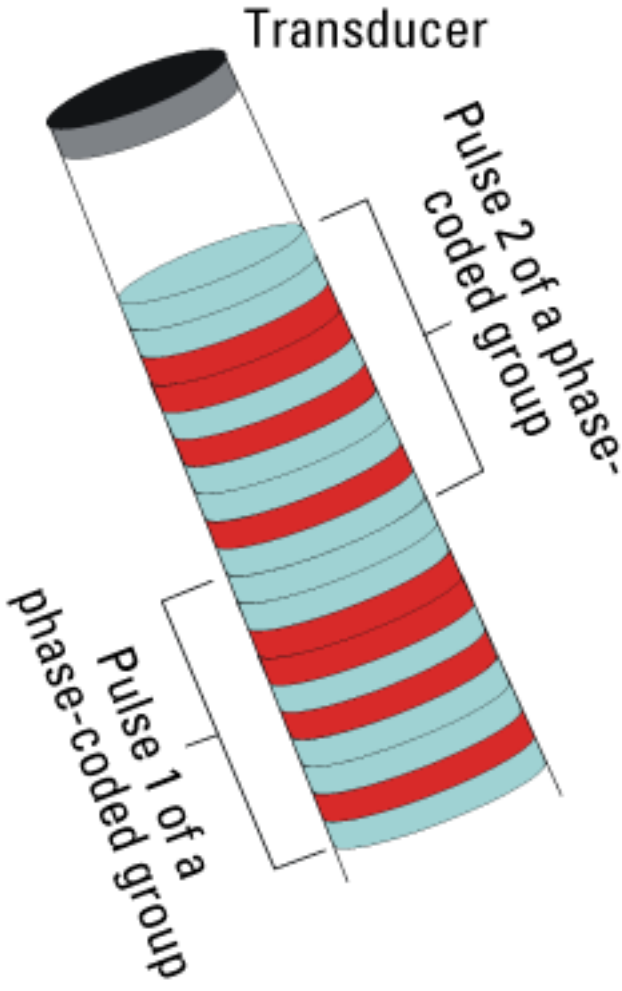


**Figure 1.39.** Phase-coded pulse pair.

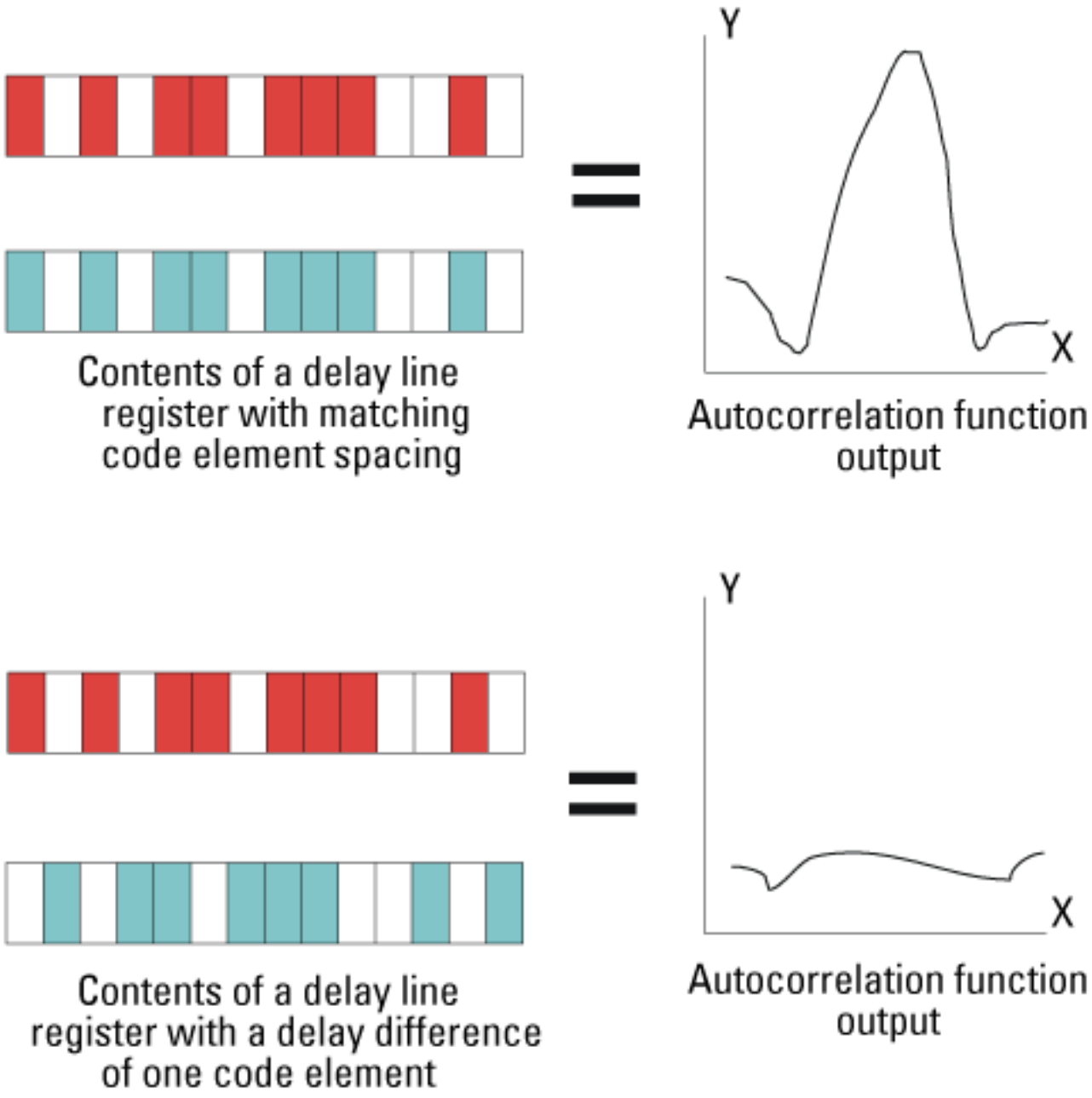


**Figure 1.40.** Effects of code element lag on correlation.

greater effective N (number of samples used for data averaging). Effective N as opposed to actual N is discussed in chapter 9. Obviously, there are times when accidental correlation occurs because currently there are only two phase choices, but, overall, a much greater precision is achieved using phase coding (because of improved signal-to-noise ratio) than by simply using a narrow pulse pair. The principle reason the manufacturers named the ADCP "broad-band" was that its bandwidth was increased to accommodate the signal processing of narrow-pulse pair (coded or not). The amount of random uncertainty in velocity measurements due to self noise has not been formally presented by the BB-ADCP manufacturer, but presumably is contained in the performance data for overall system random uncertainty (noise) values predicted by the manufacturer's error model and presented later in this chapter. When a phase coding method is used to reduce random uncertainty due to self noise, its effectiveness is greatly dependent on the order and number of the pseudo-random code elements used to construct the measurement pulse pair.

**Table 1.1.** Comparison of narrow-band and broad-band single-ping standard deviation

[m, meter; ft, foot; cm/s, centimeter per second; ft/s, foot per second]

| Property | Narrow-band | Broad-band |
|---|---|---|
| Single-ping standard deviation | 13.5 cm/s (0.44 ft/s) | 6.4 cm/s (0.21 ft/s) |
| Minimum bin size | 1. m (3.3 ft) | .25 m (.82 ft) |
| Pings per second | 8 | 2 |
| Standard deviation of a 5-second average | 2.1 cm/s (.07 ft/s) | 1.81 cm/s (.06 ft/s) |

The single-ping random error of a narrow-band ADCP is significantly higher than a BB-ADCP for a given operating frequency and bin size. However, the signal processing requirements of the BB-ADCP system are much greater than those of the narrow-band ADCP, slowing the ping rate markedly. The ping rate of a narrow-band ADCP system can be as high as 10 pings per second (or higher, depending on depth and transducer frequency), whereas the maximum ping rate of a BB-ADCP system is less than three pings per second (using present technology). Table 1.1 is an example of the net result of these effects (for 30º beam-angle systems).

The narrow-band ADCP has a 5-second average standard deviation that is comparable to the BB-ADCP if the BB-ADCP bin size is one-fourth that of the narrow-band ADCP. This means that the BB-ADCP has a higher resolution and a smaller bin size, and can be used in shallower water than the narrow-band ADCP system for a given operating frequency.

Future systems using the narrow-band ADCP technology should not be ruled out. If an adaptive scheme were used to increase the narrow-band ADCP ping rate and reduce the narrow-band ADCP bin size in shallow water, discharge measurements using either system would have comparable accuracies. Because of larger, more energetic pulses, the narrow-band ADCP system also has a slightly greater range for a given frequency than the BB-ADCP system, as well as a more robust bottom-tracking ability.

## Summary

Narrow-band acoustic Doppler current profilers (ADCPs) and broad-band acoustic Doppler current profilers (BB-ADCPs) use the Doppler principle to measure profiles of water velocity. To measure discharge, they also must measure velocity of the ADCP, relative to the river or estuary bottom.

Narrow-band ADCPs use a measurement method called pulse-to-pulse incoherent velocity measurement, which means that the ADCP transmits single, independent acoustic pulses from each beam and resolves the Doppler frequency shift during the duration of a single pulse. The frequency determination method usually is an autocorrelation technique.

BB-ADCPs use two or more coherent (synchronized) acoustic pulses in a scheme called the pulse-to-pulse coherent method. The frequency determination method usually is an autocorrelation technique that measures the phase angle difference and the time difference (spacing) between the transmitted and received pulse pairs to determine Doppler shift.

The single-ping random error of a narrow-band ADCP is significantly higher than a BB-ADCP for a given operating frequency and bin size, however, the signal processing requirements of the BB-ADCP system are much greater than those of the narrow-band ADCP, slowing the ping-rate markedly.

Increasing the lag distance between the pulse pairs in a BB-ADCP system lowers the single-ping standard deviation (to a point). Longer lag times increase the chances of ambiguity errors and should be used with caution, especially when averaging data.

# CHAPTER 2: ACOUSTIC DOPPLER CURRENT PROFILER DISCHARGE-MEASUREMENT PRINCIPLES

In chapter 1, narrow-band ADCP and BB-ADCP velocity measurements were discussed in detail. In this chapter, we will discuss the methods used to calculate discharge from data collected using an ADCP. A basic knowledge of conventional river discharge-measurement techniques is necessary to understand how an ADCP measures discharge. Conventional ADCP discharge-measurement techniques are covered in Buchanan and Somers (1969).

## Parts of an Acoustic Doppler Current Profiler Discharge Measurement

Just how is an ADCP used to measure discharge? The ADCP could be used as a conventional current meter. If an ADCP were mounted to a boat, the operator could position the boat at 30 or more stations (verticals) in the cross section. Velocities and depths could then be taken at each vertical, and the discharge calculated using the area/velocity method ($Q = AV$). Such a method would be only a slight improvement over the conventional boat-tagline discharge-measurement techniques.

The unique ability of the ADCP to continuously collect water-velocity profile data and ADCP-velocity (boat-velocity) data, relative to the bottom, lends itself to the use of a more sophisticated method of discharge-measurement integration. A velocity vector cross product at each depth bin in a vertical profile is calculated using ADCP-collected data. This cross product is first integrated over the water depth measured by the ADCP and then integrated, by time, over the width of the cross section. The following equations illustrate the integration method. The reader should try to envision them as descriptions of the discharge-measurement algorithm and mechanics.

## Velocity Cross-Product Measurement Using an Acoustic Doppler Current Profiler

### General Equation

The general equation (eq. 2.1) for determining river discharge through an arbitrary surface, $s$, is

$$Q_t = \int_s \bar{V}_f \cdot \bar{n}\, ds \qquad (2.1)$$

where

$Q_t$ = total river discharge, in cubic meters per second;

$\bar{V}_f$ = mean water-velocity vector, in meters per second;

$\bar{n}$ = a unit vector normal to $ds$ at a general point; and

$ds$ = differential area; in meters.

### The General Equation, as Applied to Acoustic Doppler Current Profiler Moving-Boat Measurements

The above is just a form of the familiar equation $Q = AV$ integrated over a cross section. For moving-boat discharge applications, the area $s$ is defined by the vertical surface beneath the path along which the vessel travels. The dot product of $\bar{V}_f \cdot \bar{n}$ will equal zero when the vessel is moving directly upstream or downstream, and will equal $\bar{V}_f$ when the vessel is moving normal to $\bar{V}_f$; both vectors are in the horizontal plane.

Because the ADCP provides vessel-velocity and water-velocity data in the vessel's coordinate system, it is convenient to recast equation 2.1 in the following form (eq. 2.2) (Christensen and Herrick, 1982):

$$Q_t = \int_0^T \int_0^d ((\bar{V}_f \times \bar{V}_b) \cdot \bar{k})\, dz\, dt \qquad (2.2)$$

where

$T$ = total cross-section traverse time, in seconds;

$d$ = total depth, in meters;

$\bar{V}_b$ = mean vessel-velocity vector, in meters per second;

$\bar{k}$ = a unit vector in the vertical direction;

$dz$ = vertical differential depth, in meters; and

$dt$ = differential time, in seconds.

The derivation of this equation by Christensen and Herrick (1982) is summarized in Simpson and Oltmann (1993). The equation originally was formulated by Kent Dienes (R.D. Instruments, Inc., oral commun., 1986).

The cross-product algorithm is well suited to ADCP discharge-measurement systems. Translated into nonmath terms, the above can be described as the cross product of the boat velocity and the water velocity first integrated over the cross-section depth and then integrated, by time, over the cross-section width (fig. 2.1).

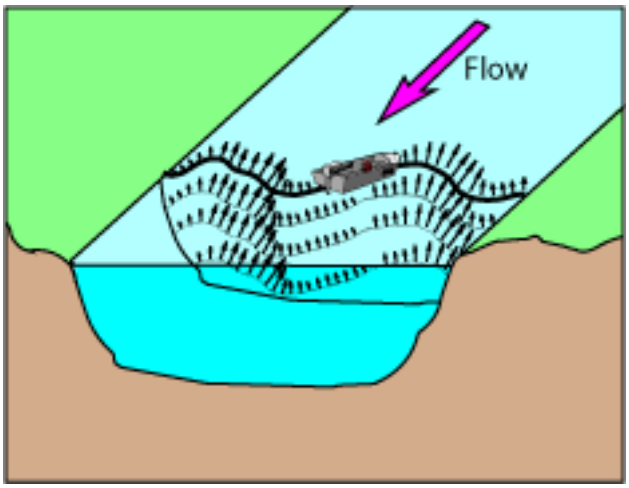


**Figure 2.1.** Cross-product vectors during a cross-section traverse.

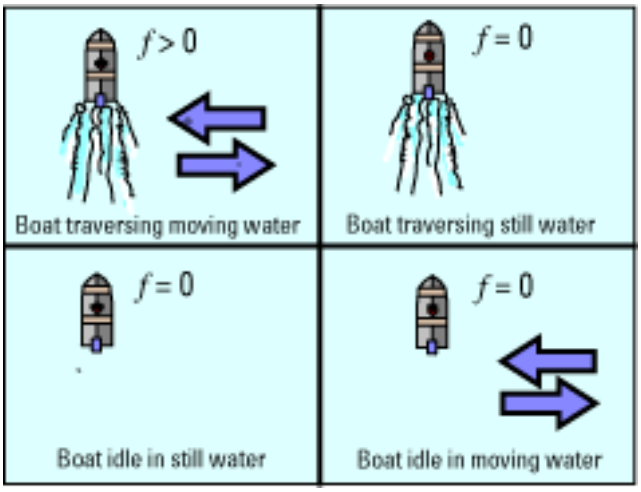


**Figure 2.2.** Properties of the water-velocity/boat-velocity cross product.

The cross product part of equation 2.2, $(\bar{V}_f \times \bar{V}_b) \cdot \bar{k}$, can be converted to rectangular coordinates to facilitate plugging in boat- and vessel-velocity vectors (eq. 2.3).

$$(\bar{V}_f \times \bar{V}_b) \cdot \bar{k} = a_1 b_2 - a_2 b_1 , \qquad (2.3)$$

where

$a_1$ = cross component of the mean water-velocity vector, in meters per second;

$a_2$ = fore/aft component of the mean water-velocity vector, in meters per second;

$b_1$ = cross component of the mean vessel-velocity vector, in meters per second; and

$b_2$ = fore/aft component of the mean vessel-velocity vector, in meters per second.

This is simply called the velocity cross product, which can be represented as shown in equation 2.4:

$$f = a_1 b_2 - a_2 b_1 , \qquad (2.4)$$

where

$f$ = the cross product of the water-velocity and boat-velocity vectors.

### Properties of the Acoustic Doppler Current Profiler Measured Cross Product

Figure 2.2 shows the properties of the cross product. Note that the boat must be traversing a velocity field before the cross product becomes greater than zero. In practice, several ADCP pings often are averaged to help reduce random error. This group of averaged water- and bottom-track velocity measurements is called an ensemble. The cross product is calculated from the averaged ensemble velocities and is expressed in units of square meters per second per second.

#### Integrating the Cross Product Over the Water Depth

When the cross product is integrated over depth, the resulting value is in cubic meters per second per second, and by substituting in the values for the beginning and ending times of each ensemble, a discharge value (cubic meters per second) is determined for each measured ensemble. The discharges for each ensemble then are summed to obtain total channel discharge (fig. 2.1). The mechanics of this operation require casting equation 2.2 into a form usable by the ADCP measurement software (eq. 2.5):

$$Q_m = \sum_{i=1}^{N_s} \left[ \int_0^d f_z \, dz \right] t_i \qquad (2.5)$$

where

$Q_m$ = measured channel discharge (doesn't include the unmeasured near-shore discharge), in cubic meters per second;

$N_s$ = number of measured discharge subsections;

$i$ = index of a subsection;

$d$ = depth of a subsection, in meters;

$f_z$ = value of cross product at depth $z$;

$dz$ = integrated vertical depth of subsection $i$, in meters; and

$t_i$ = elapsed traveltime between the ends of subsections $i$ and $i-1$, in seconds.

### Estimating Cross Products in the Unmeasured Portions of the Profile

Problems arise when trying to implement the above summation for several reasons. To understand those reasons, the limitations of an ADCP water-velocity measurement are reexamined in the following sections.

### Blanking Distance

Blanking distance was discussed in chapter 1, but is examined again here. Figure 2.3 is a modified version of figure 1.21 showing the unmeasured parts of a vertical-velocity profile. As discussed in chapter 1, the small ceramic element in the transducer is like a miniature gong. The large voltage spike of the transmit pulse bangs it like a hammer, and the vibrations, as well as the residual signal, must die off before the transducer can be used to receive incoming signals. This means that incoming signals are not used if they are received during a short period after the signal is transmitted. This time period is equivalent to a distance traveled by the signal known as the blanking distance. The blanking distance plus the transducer draft (depth of the transducer face below the water surface) compose a part of the near-surface profile that is not measured by the ADCP.

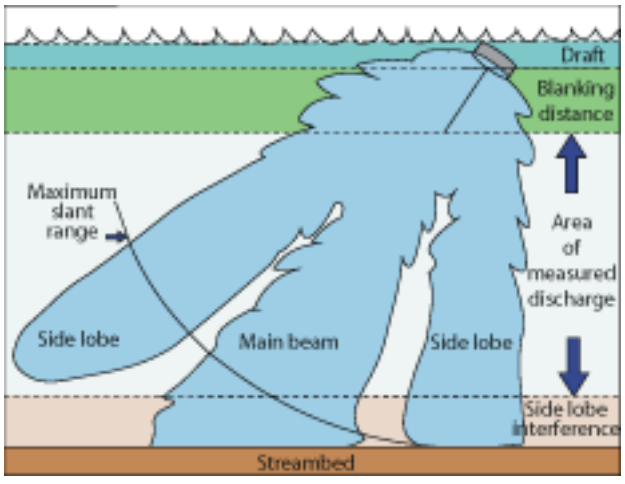


**Figure 2.3.** Acoustic Doppler current profiler-beam pattern showing side-lobe features.

### Side-Lobe Interference

Most transducers emit unwanted (parasitic) side lobes of acoustic energy at 30–40º angles off the main beam. Figure 2.3 shows a slice of a typical transducer beam pattern. The side lobe probably is a single, hollow cone with its apex at the transducer (fig. 2.4). This is only the author's mental image of the three-dimensional side-lobe structure, but the image probably is a simplistic view of the true pattern. This three-dimensional structure should be kept in mind when profiling close to obstacles. Most acoustic beams have parasitic side lobes (including external depth sounders that may be mounted on the vessel). As discussed in detail in chapter 1, up to 15 percent (depending on the beam angle) of the water column near the bottom cannot be measured because of interference from these side lobes.

The combination of the effects of transducer draft, blanking distance, and side-lobe interference yields a profile that is incomplete. To properly compute discharge for each subsection, the cross-product values near the water surface and near the bottom must be estimated.

As shown in figure 2.5, $f$ values are not provided at or near the water surface and below a point equal to 85–94 percent of the total depth. The percent of unmeasured profile area depends on the beam angle. The unknown $f$ values are labeled $f1$ at the water surface and $fn$ at the channel bottom. The simplest method of estimating these $f$ values would be to let $f1$ at the surface equal $f2$ and to let $fn$ at the bottom equal the last measured value ($fn-1$) and approximate the

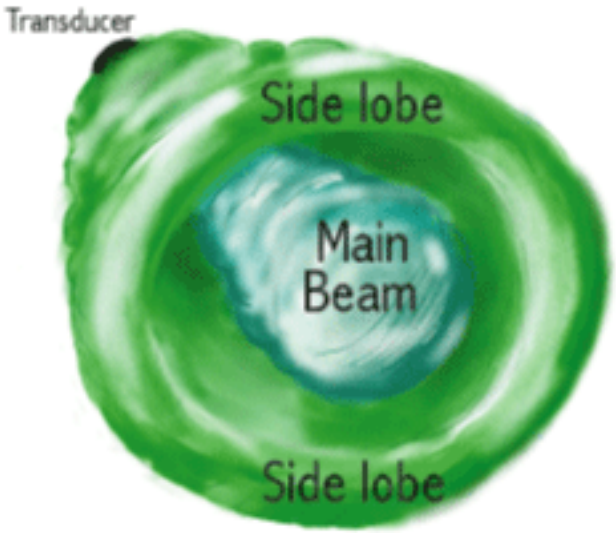


**Figure 2.4.** Hypothetical shape of a parasitic, side-lobe pattern.

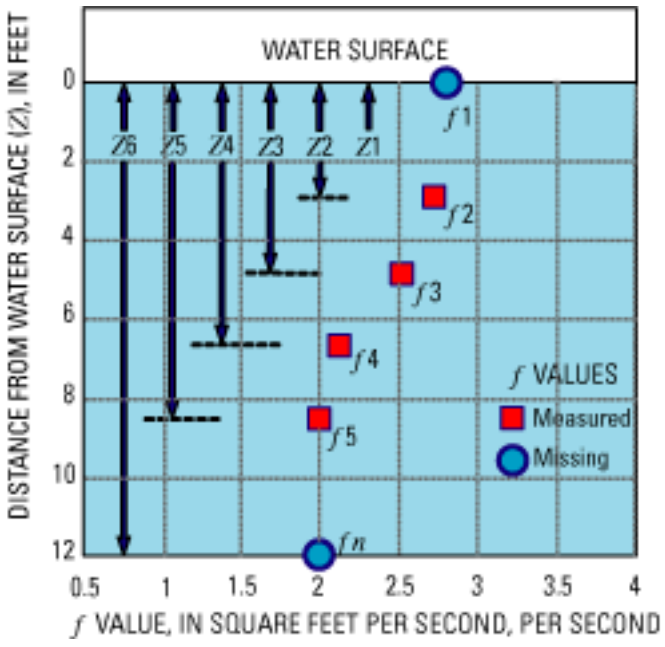


**Figure 2.5.** Example velocity profile showing measured and missing $f$ values.

integral in equation 2.5 using a trapezoidal calculation (eq. 2.6):

$$g_i = \sum_{i=1}^{n-1} \left( \frac{f_j + f_{j+1}}{2} \right) (z_{j+1} - z_j) , \qquad (2.6)$$

where

$g_i$ = depth-weighted mean $f$ value in measurement subsection $i$, in square meters per second per second;

$j$ = index of depths and respective $f$ values;

$n$ = number of measured and estimated $f$ values; and

$z_j$ = depth from water surface of respective measured and estimated $f$ values.

Although equation 2.6 appears intimidating, it is nearly the same method as used on standard USGS discharge-measurement notes to sum discharge. In this case, however, it is used from surface to bottom rather than across the width of the river.

#### Evolution of the One-Sixth Power-Curve Estimation Technique

The above method might work, but, in most cases, water at the surface is moving faster than water deeper in the profile, and the water near the bottom of the profile slows to zero velocity as it nears the channel bed (assuming a stationary bed). There are exceptions to this rule, especially in an estuary, but for general use, the top-most and bottom-most values in an ADCP-measured profile must be estimated to calculate an accurate ADCP discharge measurement.

The author attempted to calculate discharge using several different methods for profile estimation (Logarithmic and general power law), but found that because of "noisiness" of the ADCP-profile data, the resulting least-squares-derived estimates were unrealistic, especially near the upper part of the profile. A method using a one-sixth power law (Chen, 1989) eventually was chosen because of its robust noise rejection capability during most streamflow conditions. A full discussion of the one-sixth power law and its derivation can be found in Simpson and Oltmann (1993). The power law estimation scheme is an approximation only and emulates a Manning-like vertical distribution of horizontal water velocities. Different power coefficients can be used (one-half to one-tenth) to adjust the shape of the curve fit to emulate profiles measured in an estuarine environment or in areas that have bedforms that produce nonstandard hydrologic conditions and provide alternate estimation schemes under those circumstances. Figure 2.6 shows a one-sixth power curve drawn through the same set of $f$ values that were illustrated in figure 2.5.

In cases where bidirectional flow exists (water is moving one direction at the surface and is moving the opposite direction near the channel bottom), the power-curve estimation scheme will not work. In these cases, the unmeasured areas must be estimated using other methods.

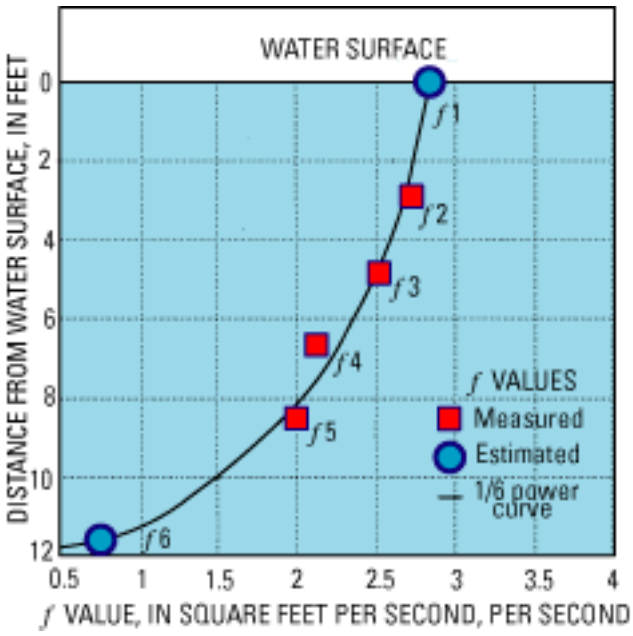


**Figure 2.6.** Example velocity profile of one-sixth power-curve fit and typical $f$ values.

In most cases, points at the top and the bottom of the profile can be estimated using the one-sixth power-curve estimation scheme. The estimated points then are used with the actual measured points, to calculate a depth-weighted mean cross product for each ensemble. Discharge then can be calculated for each ensemble pair because the time between each ensemble is known.

#### Integration, By Time, Over the Width of the Cross Section

The summation in equation 2.5 is accomplished by equation 2.7

$$q_i = g_i t_i \tag{2.7}$$

where

$q_i$ = midsection discharge between measurement subsection $i$ and subsection $l-1$, in cubic meters per second;

$g_i$ = depth-weighted mean $f$ value in measurement subsection $i$, in square meters per second per second; and

$t_i$ = vessel traveltime between measurement subsection $i$ and $i-1$, in seconds.

Equation 2.5 is used to calculate the main channel discharge by summing all $Q$ values (eq. 2.7) collected during the cross-section traverse. Unfortunately, before the total channel discharge can be calculated, two other areas need estimation schemes (fig. 2.7).

## Estimating Discharge Near the Channel Banks

The power-curve fitting scheme estimates values in the areas at the top and bottom of the profile (blanking/draft distance and side-lobe interference

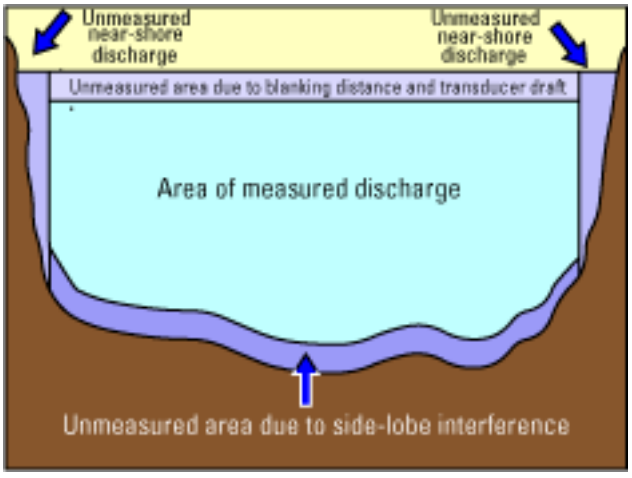


**Figure 2.7.** Unmeasured areas in a typical acoustic Doppler current profiler discharge-measurement cross section.

area), but, because of these and other ADCP depth limitations, shallow areas near the edges of the riverbank cannot be measured. The near-shore areas are estimated using a ratio interpolation method presented by Fulford and Sauer (1986), which can be used to estimate a velocity at an unmeasured location between the riverbank and the first or last measured velocity in a cross section. The equation for the estimate is equation 2.8

$$\frac{V_e}{\sqrt{d_e}} = \frac{V_m}{\sqrt{d_m}} \tag{2.8}$$

where

$e$ = a location midway between the riverbank and first or last ADCP-measured subsection;

$V_e$ = estimated mean velocity at location $e$, in meters per second;

$V_m$ = measured mean velocity at the first or last ADCP-measured subsection, in meters per second;

$d_e$ = depth at subsection $e$, in meters; and

$d_m$ = depth at the first or last ADCP-measured subsection, in meters.

Fulford and Sauer (1986) defined $d_m$ and $V_m$ as depth and velocity at the center of the first or last measured subsection and not the near-shore edge of the subsection, as presented in equation 2.8. However, because the ADCP subsections purposely are kept very narrow at the start and finish of each measurement, the differences between the two applications are not significant (Simpson and Oltmann, 1993). Figure 2.8 illustrates the estimation method used for near-shore discharge. With this method, discharge can be estimated by assuming a triangular discharge area between subsection $m$ and the riverbank, which reduces equation 2.6 to equation 2.9

$$V_e = 0.707 V_m \tag{2.9}$$

Remembering that $Q = AV$, discharge in the estimated area can be calculated by equation 2.10.

$$Q_e = \frac{0.707 V_m L d_m}{2} \tag{2.10}$$

where

$Q_e$ = estimated edge discharge, in cubic meters per second; and

$L$ = distance to the riverbank from the first or last ADCP-measured subsection, in meters.

The discharge-measurement software calculates depth ($d_m$) from the average of the depths measured on all four beams. The distance ($L$) to the riverbank from the first or last discharge measurement subsection is provided by the system operator using estimation techniques described in the chapter on discharge-measurement techniques.

The triangular ratio-interpolation method works well in parabolic-shaped natural channels, however, it does not work well in rectangular concrete channels or natural channels with nonstandard slopes near the banks. In these cases, a bank-slope coefficient can be used to properly depict the channel-bank geometry (see chapter 5.)

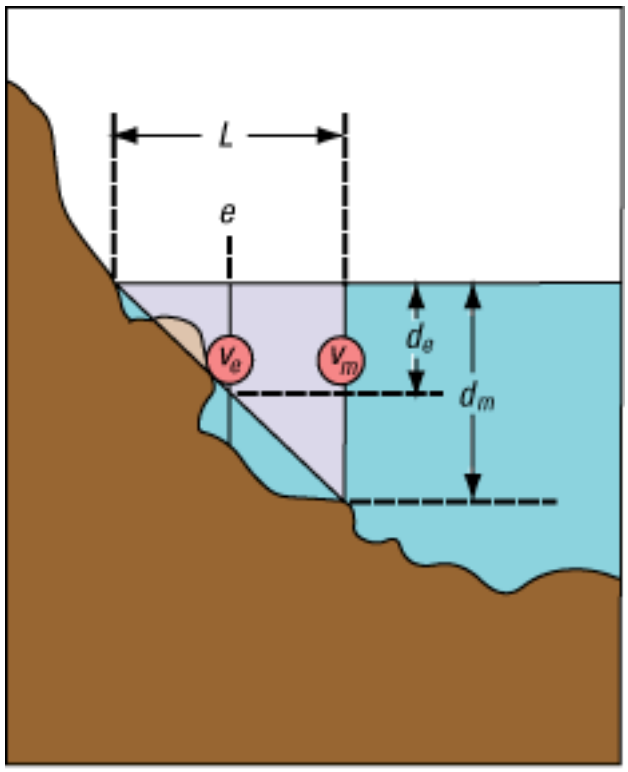


**EXPLANATION**

| | |
|---|---|
| $v_e$ | Estimated mean velocity at location $e$ |
| $v_m$ | Measured mean velocity at first or last ADCP-measured subsection |
| $d_e$ | Depth at subsection $e$ |
| $d_m$ | Depth at first or last ADCP-measured subsection |
| $L$ | Distance to the riverbank from the first or last ADCP-measured subsection |
| $e$ | A location midway between the riverbank and first or last ADCP-measured subsection |

**Figure 2.8.** Edge-value estimation scheme described by equations 2.8, 2.9, and 2.10. ADCP, acoustic Doppler current profiler.

## Determination of Total River Discharge—Putting it All Together

Using all the methods and equations described in this chapter, total river discharge ($Q_t$) can be calculated by equation 2.11

$$Q_t = Q_m + Q_{e_i} + Q_{e_r} \quad (2.11)$$

where

$Q_m$ = total channel discharge [the sum of all $q_i$ values collected during the discharge measurement traverse (eq. 2.7)], in cubic meters per second;

$Q_{e_i}$ = near-shore discharge estimate on the left side of the channel, in cubic meters per second; and

$Q_{e_r}$ = near-shore discharge estimate on the right side of the channel, in cubic meters per second.

## Discharge-Measurement Software

Based on the above principles, the USGS, as well as the manufacturers of ADCPs, have written computer programs designed to collate ADCP data collected during a cross-section traverse and compute discharge in real time. Because of the difficulty in maintaining and updating such a program, the USGS has elected to use manufacturers' proprietary programs for this capability, provided the proper algorithms are used and quality assurance (QA) criteria are met. The current QA plan (Lipscomb, 1995) requires that the whole system (ADCP and discharge-measurement software) meet certain standards.

The USGS has an archtype computer program written in Pascal that can be used as a basis for a vendor-created software package. Because the archtype computer program has not been translated into machine code that will run on IBM personal computers and compatibles, most ADCP system operators utilize "Transect," a suite of proprietary software modules developed by RDI for use with their ADCPs. The

Transect software includes the estimation methods used by the USGS in the archtype program and has proven to be a useful, accurate discharge-measurement tool. Other manufacturers currently are developing similar software.

## Summary

Unlike conventional discharge-measurement methods, acoustic Doppler current profiler (ADCP) discharge-measurement software does not calculate discharge directly from area and velocity data. The ADCP discharge-measurement software calculates a water/boat velocity vector cross product in each bin before integrating the cross products over the sub-section depth. The resulting subsection discharges then are summed over the width of the cross section.

Discharge cannot be measured near the water surface because of the draft required by the transducer (depth below water surface) and transducer blanking distance. Discharge cannot be measured near the channel bed primarily due to side-lobe interference. Cross products in these unmeasured portions of the channel cross-section usually are estimated using a one-sixth power-curve estimation scheme (unless the profile shape dictates other methods). Discharges in the unmeasured portions of the cross-section near the edges of the riverbank are estimated using a ratio-interpolation method.

The U.S. Geological Survey (USGS) has developed a discharge-measurement archtype program; however, most ADCP system operators are using a proprietary suite of software modules called “Transect” developed by R.D. Instruments, Inc., for use with their ADCPs. Transect includes the estimation methods used by USGS in the archtype program and has proven to be a usable, accurate discharge-measurement tool. Other manufacturers also are developing discharge-measurement software.

This page left blank intentionally.

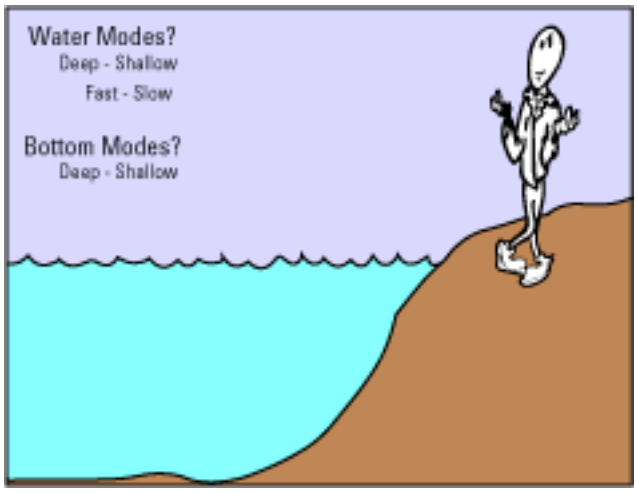


**Figure 3.1.** Choosing the proper measurement mode is difficult.

# CHAPTER 3: R.D. INSTRUMENTS, INC., BROAD-BAND ACOUSTIC DOPPLER CURRENT PROFILER MEASUREMENT MODES

## Measurement Modes—Why?

One of the most compelling features of ADCP systems is their versatility. Versatility comes with a cost, however, and the cost is added complexity. Most ADCPs have several water-measurement modes (fig. 3.1) and bottom-measurement modes. These modes are chosen based on environmental conditions (fast/slow or shallow/deep water and current shear). A simple matrix of mode choices for different measurement conditions would be desirable for this chapter, but, unfortunately, it's not that easy! Several environmental factors may play a part in the choice of measurement modes.

In an ADCP manufactured by RDI, these modes are set using direct commands placed in a configuration file (chap. 5). The BB-ADCP commands W (water mode) and B (bottom mode) can be set to different values depending upon the flow and bottom conditions expected at the discharge measurement site. Mistakes in setting these values may cause unrecoverable errors in the measurement of discharge. This chapter, therefore, is devoted to the explanation of the different operational modes available for ADCPs manufactured by RDI. It is quite likely that when this report is published, operational modes for ADCPs manufactured by RDI will be available that are not covered in this chapter. The manufacturer releases technical notes and bulletins when such changes are developed, which are available on the manufacturer's web site (www.rdinstruments.com).

Parameters that dictate the operation of water- and bottom-track measurement modes are set by direct commands sent to the profiler from the Transect configuration file (chap. 5). These direct commands take the form of W$nnn, or B$nnn, where W = water mode and B = bottom mode. The "$" signifies the water- or bottom-mode parameter that receives the numeric value, nnn. These direct commands are discussed in detail in this chapter.

## Water Modes

The water-measurement modes juggle different lag distances, pulse lengths, code element combinations, and adaptive schemes to measure water velocity under many hydrologic conditions. Some of these modes should be used with caution because errors can result if they are misapplied. Direct commands for these modes take the form of WMn, where n is 0, 1, 4, 5, 7, or 8, depending on the mode used.

### Water Mode Zero (WM0)

Water mode zero (direct command WM0) is referred to as the "expert" mode because it allows the user to set virtually all aspects of the water-measurement ping structure. Water mode zero will not be addressed further in this report because it is almost never used under routine measurement conditions. When this mode is used, it is used in connection with instructions from the manufacturer and usually is used for special circumstances where other modes are inadequate.

### Water Mode 1 (WM1)

Water mode 1 (direct command WM1) is called the "dynamic" mode. This is a general purpose mode that should be used (in preference to mode 4) for most routine measurement conditions—with one caveat; the ambiguity velocity must be set correctly for stream conditions. Operators can modify the ambiguity velocity (and, thereby, the lag spacing of the mode 1 ping structure) using the WV command. Proper adjustment of the WV value allows mode 1 to be used in shallow and deep water and in current shear where other modes fail. Ambiguities in the measurement of velocity are not automatically resolved in water mode and the maximum expected velocity of the boat (relative to the water) must be estimated before setting the WV command. If the value is set too low, an ambiguity error could be introduced into the velocity measurement (see chap. 1).

The default WV value (lag spacing) for mode 1 allows a high ambiguity velocity [480 centimeters per

second (cm/s), 16 ft/s]. The single-ping standard deviation of a velocity measurement using this default setting is about 19 cm/s (0.62 ft/s). This magnitude of uncertainty usually produces an unacceptable precision for the resulting discharge measurement, unless the measurement vessel is slowed to less than one-third of the speed of the absolute water velocity (water velocity relative to the Earth) during the cross-section traverse. Fortunately, the mode 1 default lag spacing can be changed by altering the WV command. Note: Most of the ambiguity-velocity directives expect radial (along-beam) ambiguity velocity, not horizontal ambiguity velocity. Radial ambiguity velocity can be determined using the following formula (eq. 3.1) if the desired horizontal ambiguity velocity is estimated

$$V_{radial} = 1.5(V_{horizontal})\sin\theta \qquad (3.1)$$

where

$V_{radial}$ = radial ambiguity velocity, in centimeters per second;

$V_{horizontal}$ = horizontal ambiguity velocity, in centimeters per second; and

$\theta$ = transducer beam angle, in degrees.

The horizontal ambiguity velocity can be estimated by adding the highest expected ADCP speed (relative to the water) and the highest expected absolute water velocity. This value is $V_{horizontal}$ and is plugged into equation 3.1 to arrive at a reasonable value for the WV command. It is multiplied by 1.5 in the equation for safety reasons. Usually, it is better to have a bit of extra noise (standard deviation of velocities) in the measurement than to inadvertently average in an ambiguity error. Table 3.1 shows the single-ping standard deviation for three different ambiguity-velocity values.

Mode 1 can be used in slightly more shallow water than mode 4 [1 m (3.3 ft)], but modes 5 or 8 are preferred for medium-to-slow velocities [below 10 cm/s (0.33 ft/s)] because of the increased resolution available with these modes. Mode 1 sometimes can be used in shallow water where modes 5 and 8 do not work because of high velocities and shear. Figure 3.2 shows the depth and velocity range windows wherein each mode is designed to function properly. Notice that mode 1 encompasses a much larger range of depths and velocities than do the other modes.

To increase the range of mode 1 in water depths near the edge of the ADCP measurement capability (depends on frequency), the operator can toggle the WB command from 0 to 1. According to the manufacturer, setting the WB command to 1 enables greater ADCP range by narrowing the received bandwidth (which improves the signal-to-noise ratio). Unfortunately this also increases the velocity measurement standard deviation by a factor of 2. See chapter 9 (table 9.1) for the maximum recommended ranges for ADCPs of different frequencies. The WB command only can be used for mode 1 operation. Setting WB to anything other than zero in other water modes will cause unpredictable results.

For routine discharge measurements in swift-flowing waters with depths greater than 2 m (6.5 ft), mode 1 is the mode of choice. The operator must set the WV command for the proper ambiguity velocity. Water

**Table 3.1.** Mode 1 single-ping standard deviation using three different values for the WV command

[ADCP, acoustic Doppler current profiler; kHz, kilohertz; cm/s, centimeter per second; ft/s, foot per second]

| ADCP frequency (kHz) | Ambiguity velocity (WV command) | Single-ping standard deviation |
|---|---|---|
| 300 | 480 cm/s (15.78 ft/s) | 19.35 cm/s (0.63 ft/s) |
| 300 | 190 cm/s (6.23 ft/s) | 14.07 cm/s (.46 ft/s) |
| 300 | 60 cm/s (1.99 ft/s) | 6.87 cm/s (.23 ft/s) |
| 600 | 480 cm/s (15.78 ft/s) | 19.35 cm/s (.63 ft/s) |
| 600 | 190 cm/s (6.23 ft/s) | 14.08 cm/s (.46 ft/s) |
| 600 | 60 cm/s (1.99 ft/s) | 6.87 cm/s (.23 ft/s) |
| 1200 | 480 cm/s (15.78 ft/s) | 19.37 cm/s (.64 ft/s) |
| 1200 | 190 cm/s (6.23 ft/s) | 14.08 cm/s (.46 ft/s) |
| 1200 | 60 cm/s (1.99 ft/s) | 6.87 cm/s (.23 ft/s) |

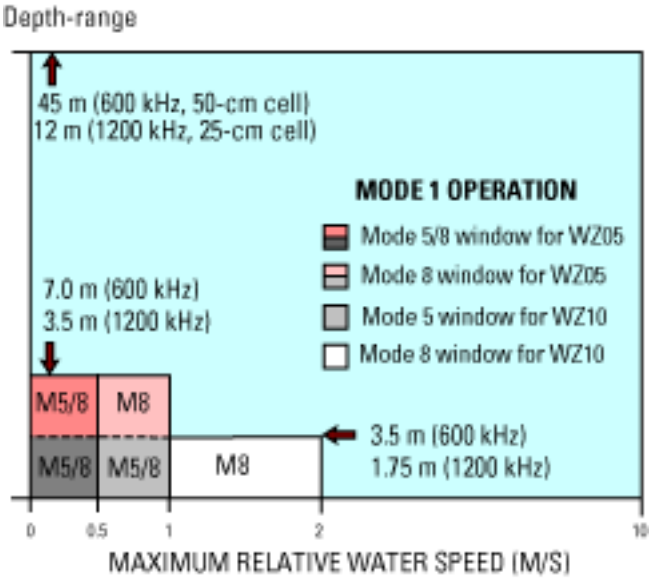


**Figure 3.2.** Depth/range/speed-operational "windows" for water modes 1, 5, and 8. m, meter; kHz, kilohertz; cm, centimeter; M/S, meter per second.

modes 2 and 3 are obsolete and are no longer used for riverine measurements.

#### Water Mode 4 (WM4)

Until recently, water mode 4 (default for the BB-ADCP) was used as the general production mode for water-discharge measurement. This mode is no longer recommended by RDI for discharge measurement because of hard-to-detect errors that can be introduced with automatic mode switching. Mode 4 uses a single set of pulses with a long lag that is dependent on depth cell length. The lag is either one-half the depth cell length or has a horizontal ambiguity velocity of 160 cm/s (5 ft/s), whichever is greater. The value of 160 cm/s (5 ft/s) is used for most depth cell sizes. Using the minimum depth cell size for a given operational frequency [25 centimeters (cm), 10 inches (in.)] for a 1,200-kHz BB-ADCP, for example, will decrease the lag, raise the ambiguity velocity slightly, and increase the measured water-velocity standard deviation. The ambiguity is resolved on this single set of pings by a proprietary signal-processing algorithm developed by the manufacturer (R.D. Instruments, Inc., 1996).

If necessary, mode 4 can be used in high- and low-velocity conditions. When depths become too shallow [2 meters (m) and below], or if the signal return is too weak, the ADCP will shift automatically to mode 1 operation. The operator is not notified when automatic mode switching occurs and it is recommended that an appropriate WV command be inserted into every configuration file that uses mode 4 operation. The WV command value can be estimated using equation 3.1 (see Water Mode 1 discussion).

Again, mode 4 is no longer recommended for discharge measurement use. It is only available on BB-ADCP systems and should be used only if directed by the manufacturer, or if mode 1 will not work.

#### Water Mode 5 (WM5)

Water mode 5 ("low and slow" mode) uses a true version of pulse-to-pulse coherent signal processing. The two transmitted pulses are completely independent of each other, but are synchronized in phase. To eliminate self noise in mode 5, the second pulse is not sent until the first pulse dies out. This procedure creates a long lag with low standard deviation of the measured water velocity.

##### Ambiguity Velocity Revisited

One problem with extra long lags is a low ambiguity velocity. Using the racetrack analogy from chapter 1, the first strobe flash (analogous to an acoustic pulse) shows the car with the racing stripe leading the pack of racers (fig. 1.34a). The second strobe flash reveals that the pack of racers apparently has passed the racing-striped car and won the race (fig. 1.34b). Or does it? If the racing-striped car was actually moving three or four times faster than the other racers, it not only won the race but has almost "lapped" the rest of the racers. In this case, the racing-striped car has exceeded the velocity at which the timekeeper could determine its speed without ambiguity. In the case of mode 5 operation, this ambiguity velocity is relatively low [50 cm/s (1.7 ft/s) ADCP speed, relative to the water].

A long lag time increases the possibility of decorrelation between pulses. Using the above racetrack analogy, the photographer could overlay the negative of the first strobe flash on the negative of the second strobe flash and then rotate the negatives until the "pack" of cars are aligned. When the pack of cars are aligned, the checkered flag on the first negative will be a certain distance from the checkered flag on the second negative. By using this distance and the time between strobes, the speed of the pack of cars can be computed. This method of speed computation works unless the time between strobes becomes so long that the cars in the pack change position, lanes, or speeds. If this happens, the cars will not "match up" when the negatives are rotated. The two negatives are then said to be uncorrelated. This effect can occur using mode 5 if there is shear and turbulence in the water column.

Because of the above two effects, mode 5 is not usable in water with substantial velocity, shear, or turbulence. However, in slow-moving water with little current shear, mode 5 can be used to obtain highly precise discharge measurements. Because of the high precision of mode 5, smaller bin lengths can be used, which enables mode 5 to be used in shallow water. Direct command changes must be made for mode 5 operation. The WZ command sets the starting length of the mode 5 and mode 8 lags and it is recommended that a command of WZ05 be used as a starting point for mode 5 and mode 8 operation. Table 3.2 describes water mode 5 performance for the specified setup.

#### Water Mode 7 (WM7)

Water mode 7 (extended range mode) is used to obtain water profiling at ranges 10–15 percent greater than profiling ranges available in other modes. Mode 7 converts the BB-ADCP system to a system similar to a narrow-band ADCP, thereby increasing the signal-to-noise ratio and range. This mode is practical only for 75-, 150-, and 300-kHz BB-ADCPs and is intended for open-ocean use where extended depth range is needed. Mode 7 water-velocity measurements have

**Table 3.2.** Setup and performance values for water mode 5 operation (WZ05)

[kHz, kilohertz; cm, centimeter; cm/s, centimeter per second; m, meter; ft/s, foot per second; ft, foot. WF, WS, keyboard commands]

| Acoustic Doppler current profiler operating frequency (kHz) | Blanking distance WF, (cm) | Depth cell size, WS (cm) | Single-ping standard deviation (cm/s) (ft/s) | Range to first depth cell (m) (ft) | Minimum profiling range (m) (ft) | Maximum profiling range (m) (ft) |
|---|---|---|---|---|---|---|
| 600 | 25 (WF25) | 10 (WS10) | 0.5 cm/s (0.16 ft/s) | 0.35 m (1.15 ft) | 0. 9 m (2.95 ft) | 7.0 m (23.0 ft) |
| 600 | 25 (WF25) | 25 (WS25) | .3 cm/s (.010 ft/s) | .50 m (1.64 ft) | 1.6 m (5.25 ft) | 7.0 m (23.0 ft) |
| 600 | 25 (WF25) | 50 (WS50) | .2 cm/s (.007 ft/s) | .75 m (2.46 ft) | 2.2 m (7.18 ft) | 7.0 m (23.0 ft) |
| 1200 | 25 (WF25) | 5 (WS05) | .6 cm/s (.020 ft/s) | .30 m (.98 ft) | .8 m (2.63 ft) | 3.5 m (11.5 ft) |
| 1200 | 25 (WF25) | 10 (WS10) | .4 cm/s (.013 ft/s) | .35 m (1.15 ft) | .9 m (2.95 ft) | 3.5 m (11.5 ft) |
| 1200 | 25 (WF25) | 25 (WS25) | .3 cm/s (.010 ft/s) | .50 m (1.64 ft) | 1.6 m (5.25 ft) | 3.5 m (11.5 ft) |

approximately 2.5 times the standard deviation of velocities measured with a mode 4 ping using the same depth cell size.

#### Water Mode 8 (WM8)

Water mode 8 is for shallow water and will sometimes work in conditions where mode 5 will not. This mode uses a pulse-to-pulse coherent configuration much like mode 5 to calculate velocity, but employs sophisticated signal processing techniques to reduce lag times. A mode 8 ping has a single-ping standard deviation 10 times greater than a mode 5 ping of the same bin size, but can be used in shallow water in much the same manner as mode 5. Setups for mode 8 are the same as the setups for mode 5. Table 3.3 gives the conservative values provided by the manufacturer for mode 8 performance (R.D. Instruments, Inc., 1995). Under certain circumstances, the operator may see up to a 30 percent improvement over the maximum depth range and maximum velocities listed in table 3.3; however, it is best not to expect optimum performance under field conditions.

#### Range/Speed "Windows" for Water Modes 1, 5, and 8

Figure 3.2 shows a graphic rendition of the depth-range/speed operational "windows" for water modes 1, 5, and 8. Notice that mode 1 is, by far, the most robust operational mode, with the largest operational range of depth and relative water speed. For slow velocities with shallow depths, mode 5 is the mode-of-choice, especially with 600-kHz ADCPs. Mode 8 sometimes will work in shallow water where relative water velocities are too high for mode 5 operation. The higher standard deviation of the mode 8 measurements usually requires some data averaging, or a slow cross-section traverse (at speeds below that of the water speed, relative to the Earth).

### Bottom-Track Modes

Bottom-track modes are implemented independently of the water-velocity measurement modes and sometimes are set differently. There are two bottom-track modes currently used by the BB-ADCP: modes 4 and 5. Bottom-track modes 1–3 are obsolete. Other bottom-track modes may be available by the time this report is published.

Bottom tracking is done by proprietary firmware schemes built into the ADCP by the manufacturer; however, all such schemes must rely on the assumption that the bottom reflection obeys basic laws of physics. These principles of bottom tracking should be known by the ADCP operator to properly evaluate bottom tracking under variable field conditions.

#### The Bottom Reflection

When an acoustic signal strikes the river bottom, the reflected signal normally is much stronger (by orders of magnitude) than the reflected signal from scatterers in the water mass. It is no surprise, therefore, that the standard deviation of the bottom-track velocity measurement is about 10 times less than the water-mass

**Table 3.3.** Setup and performance values for water mode 8 operation (WZ05)

[kHz, kilohertz; cm, centimeter; cm/s, centimeter per second; m, meter; ft/s, foot per second; ft, foot. WF, WS, keyboard commands]

| Frequency (kHz) | Blanking distance WF (cm) | Depth cell size, WS (cm) | Single-ping standard deviation (cm/s) (ft/s) | Range to first depth cell (m) (ft) | Minimum profiling range (m) (ft) | Maximum profiling range (m) (ft) |
|---|---|---|---|---|---|---|
| 600 | 25 (WF25) | 10 (WS10) | 8.2 cm/s (.27 ft/s) | 0.35 m (1.15 ft) | 0.6 m (1.97 ft) | 7.0 m (23.0 ft) |
| 600 | 25 (WF25) | 25 (WS25) | 5.2 cm/s (.17 ft/s) | .50 m (1.64 ft) | .9 m (2.95 ft) | 7.0 m (23.0 ft) |
| 600 | 25 (WF25) | 50 (WS50) | 3.7 cm/s (.12 ft/s) | .75 m (2.46 ft) | 1.4 m (4.59 ft) | 7.0 m (23.0 ft) |
| 1200 | 25 (WF25) | 5 (WS05) | 11.0 cm/s (.36 ft/s) | .30 m (.98 ft) | .5 m (1.64 ft) | 3.5 m (11.5 ft) |
| 1200 | 25 (WF25) | 10 (WS10) | 7.8 cm/s (.26 ft/s) | .35 m (1.15 ft) | .6 m (1.97 ft) | 3.5 m (11.5 ft) |
| 1200 | 25 (WF25) | 25 (WS25) | 5.0 cm/s (.164 ft/s) | .50 m (1.64 ft) | .9 m (2.95 ft) | 3.5 m (11.5 ft) |

velocity measurement. Figure 3.3 shows a 1,200-kHz ADCP backscattered intensity (measured in counts) that decreases with depth until the acoustic beam strikes the river bottom at a depth of approximately 7 m (23 ft). Data averaged from a series of water-track pulses were used to construct figure 3.3, but a single bottom-track pulse backscattered-intensity plot would look much the same.

Modern bottom-track schemes are self adaptive to stream conditions and use factors such as correlation magnitude, correlation side peak location, and (or) spectral width to determine the presence of the bottom echo. Still, bottom-track failures can occur when one or more of the parameter identification criteria are not met by the output signal or, for some reason, are met at the wrong time.

In the case of heavy sediment load, which causes high absorption and scattering of the acoustic signal, the weakened bottom reflection (from deep water) cannot activate a detection threshold. In some cases, when this happens, the ADCP firmware is programmed to try other (more robust) bottom-tracking modes before flagging the data as “bad.”

Another problem occurs during periods of high flow when heavy sediment loads are moving on or near the channel bed; the bottom-track velocities become biased. The physical process that causes this phenomenon is theorized only at this time. Attempts have been made to overcome this bias problem by using lower frequency systems and special bottom-track schemes. A separate method of measuring vessel velocity that eliminates the need for bottom tracking can be used; the input from a differential global positioning systems (GPS) receiver and depth sounder is used to replace the data from the ADCP bottom-track pulse. Because this method requires that the operator have an indepth understanding of GPS systems, as well

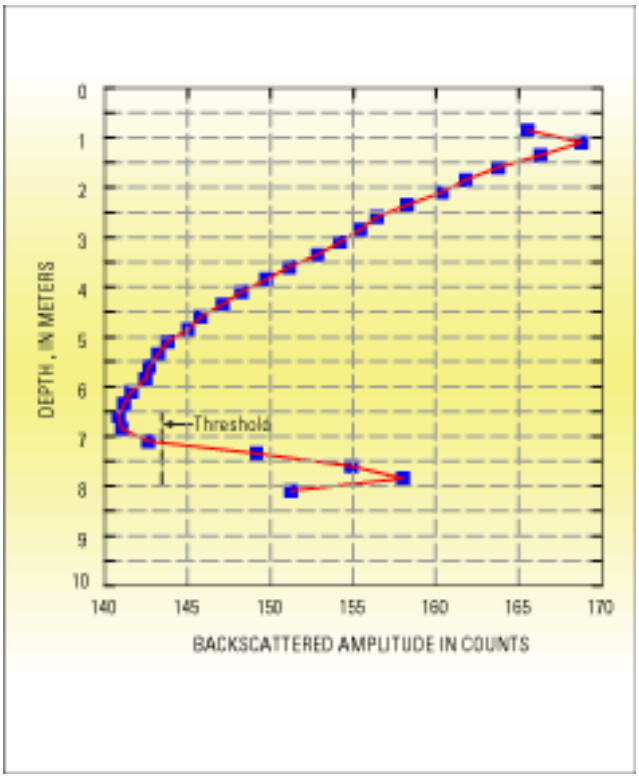


**Figure 3.3.** Acoustic Doppler current profiler-backscattered intensity with depth showing the bottom reflection.

as significant investment in additional GPS and depth sounding equipment, it will not be discussed in this report. For more information on using this method for discharge measurements during conditions of bottom-sediment movement, contact the ADCP manufacturer.

### Bottom-Track Mode 4 (BM4)

Bottom-track mode 4 is a general-purpose bottom-track mode. This mode can unambiguously determine the speed of the ADCP, relative to the channel bottom, under most conditions. The detailed detection scheme used is proprietary and copyrighted by RDI, but mode 4 uses the correlation side-peak position to resolve velocity ambiguities and it lengthens the lag at predetermined depths to improve variance. Bottom-track mode 4 can be used with water-track modes 1, 4, 5, 7, and 8; however, because of processing limitations, the standard deviation of bottom-track velocity data (using mode 4) increases as depth decreases.

### Bottom-Track Mode 5 (BM5)

Bottom-track mode 5 is the default mode for most discharge-measurement and velocity-profiling use. This mode uses a pulse-to-pulse coherent technique that has a lower variance in shallow water than bottom-track mode 4 by a factor of up to four. In very shallow water at slow speeds, mode 5 variance is lower than mode 4 by a factor of 100. Although mode 5 has a very precise measurement capability, it has a slightly slower ping rate than mode 4. Bottom-track mode 5 will automatically switch to bottom-track mode 4 when water is too deep (or too fast) for mode 5 operation. Because of this adaptive capability, mode 5 is the mode of choice for small rivers and estuaries (table 3.4). Table 3.4 lists the minimum bottom-tracking depths for bottom-track modes 4 and 5.

**Table 3.4.** Minimum depth ranges for bottom-track modes 4 and 5

[kHz, kilohertz; m, meter; ft, foot]

| Frequency (kHz) | Depth (m) (ft) |
|---|---|
| 1200 | 0.8 m (2.6 ft) |
| 600 | .8 m (2.6 ft) |
| 300 | 1.5 m (5 ft) |

At least one other ADCP manufacturer has developed the software and system firmware (bottom-tracking algorithms) for the measurement of river discharge; however, at the time this report was written, no detailed information was available for analysis and publication.

## Summary

Water-track modes and bottom-track modes are independent of each other and must be carefully chosen, depending upon the stream conditions. In general, a good starting point for measurements at an unfamiliar site is water mode 1 (WM1) and bottom-track mode 5 (BM5). In cases of slow-moving, shallow flow, water mode 5 should be tried first, followed by water mode 8, followed by modified versions of mode 1 (use bottom-track mode 5 in all cases). In cases of high velocities, high shear, abrupt boat movements, or dynamic depth conditions, default and modified versions of mode 1 can be tried with a slow cross-section traverse to reduce random error. In such cases, bottom-track mode 4 probably should be used.

The theory of ADCP discharge measurement has been discussed in chapters 1–3. Chapters 4–9 introduce “practical” techniques and equipment.